CHAPTER 1

WEATHERING THE CHANGE: MODELING CROP CHOICES IN RESPONSE TO CLIMATE VARIABILITY

1.1 Introduction

As weather patterns become more variable under climate change, the suitability of crops traditionally grown in specific regions may shift (Hoang et al., 2022; Heikonen et al., 2025). As crop-specific heat and moisture requirements vary, climate change will impact crops differently. Water-intensive crops may no longer thrive in regions experiencing drier conditions, whereas heat and drought-tolerant varieties may become more viable. The change in weather patterns will potentially alter crops' comparative advantages. Under such circumstances, sticking to traditional cropping patterns can lead to substantial losses as lower productivity will translate into lower profits. To mitigate these losses, farmers are likely to switch to crops better suited to the changing climate (Rising and Devini, 2020; Sloat et al., 2020), reshaping land use and regional production portfolios. This, in turn, can have significant market and welfare implications.

The role of climate change in driving land-use changes and producer adaptation strategies is a relatively understudied topic. Recent studies have investigated farmers' adaptations to climate change, but most have been conducted at an aggregated (i.e. county or state) (Rising and Devini, 2020; Mu et al., 2017) or very localized scale (Moniruzzaman, 2015; Ahmed et al., 2023). One major challenge in quantifying farmers' adaptation, particularly through crop choices, is the scarcity of field-level data. Crop choices or adaptation decisions are made at the field-level by farmers, but such data is often unavailable (McCarl et al., 2016). Studies relying on county- or state-level data fail to capture the granularity of decision-making and localized studies based on surveys of a small number of farmers may not be able to capture the heterogeneity of cropping decisions across different regions and conditions.

Another challenge in credibly identifying farmers' adaptations to climate change is the complex interaction between weather patterns and market conditions. Weather and field productivity influence crop yields and, ultimately, profits. Farmers base crop choices on expected profits, yet

many studies inaccurately assume constant profitability under climate scenarios (Moniruzzaman, 2015; Cui, 2020). Some studies incorporate impact of changing profitability under climate change on crop choices using two-step modeling approaches which first simulate future yields and profits and, then predict optimal crop choices based on these simulated profits (Arora et al., 2020; Rising and Devini, 2020). However, because of a lack of data on field-level profits, these studies use aggregated measures such as county or state-level profits or prices, which introduce measurement error and may underestimate the impact of profitability on crop choices.

In this paper, we rigorously investigate the factors that determine farmers' cropping decisions and how exogenous shocks, specifically climate and market conditions, affect crop choices. We provide robust evidence of adaptation through crop switching using a two-step approach. First, we estimate crop-specific yield-weather models for five crops including maize, soybean, sunflower, wheat, and rapeseed using field-level yield data. We regress crop-specific yields on 3°C temperature bins representing hours of exposure and soil moisture during different growth stages using two-way fixed effects estimation. The goals of the yield-weather model are twofold; to provide us with crop-specific thresholds of extreme weather and to allow us to predict how yields change under climate change. We then identify the key variables influencing farmers' cropping decisions by integrating the yield model results into a panel conditional logit crop choice model that utilizes field-level data on farmers' crop choices. The model is used to predict how farmers adjust their crop choices in response to climate change. Our approach provides robust and credible estimates of how farmers adjust their crop choices in response to climate change and how these changes translate into land-use reallocation at scale and farmer welfare.

This paper addresses key gaps in the literature on climate adaptation in agriculture. Our primary contribution is credible, aggregate predictions of how crop choices adjust under climate change. These predictions improve on the previous literature for three reasons. First, we develop an innovative crop choice model that effectively integrates climatic, hydrological, and economic factors to precisely capture the decision-making processes of farmers. Crop choices depend on several factors that are too often ignored in the traditional crop choice models, including variables

such as yield-specific profit and field-level irrigation status that are either excluded or proxied by other variables in the past literature (Seo and Mendelsohn, 2008). By including these variables, we characterize a crop choice model that is more closely aligned with farmers' decision-making processes in the real world. Additionally, we include both short and long-term weather in our crop choice model. Previous literature has often only included short-term weather fluctuations, as recent weather events are more likely to shape farmers' crop choices (Ahmed et al., 2023; Seo and Mendelsohn, 2008). We believe that while recent weather events affect crop choices in an obvious manner, farmers often base their expectations of weather based on long-term climatic trends.

Second, the integration of findings from yield-weather models into the crop choice model is a relatively new approach. Incorporating yield results within our profit estimates in the crop choice model improves the measurement of profit's impact on crop choices. Additionally, re-estimating yields under climate change allows us to capture the intricate relationships between productivity, crop profits and crop choices that are often overlooked in the literature.

Finally, having field-level data on crop yields and crop choices spread across an entire country is a significant improvement over the previous literature that has been conducted at an aggregated county-level. Our analysis is one of the few high-resolution studies providing us with significant heterogeneity across farmers' decisions and field characteristics that is often lost in aggregation.

The results from our yield-weather models reveal crop-specific thresholds for all five crops considered in our analysis. Using heat and cold thresholds for all spring crops including maize, soybean and sunflower, we find the heat-stress threshold to be 34°C and cold-stress threshold to be 4°C for spring crops. For winter wheat and rapeseed, we find an extreme heat threshold of 28°C and an extreme cold threshold of -5°C. Our simulations also indicate that yields change significantly under the future climate scenarios with projected decline of 8% for maize from 2040-2070 and increase of 2-3% for soybean, wheat and sunflower.

Next, we estimate a crop choice model using a panel conditional logit structure to determine the factors that play a significant role in driving farmers' crop choices. We find extreme weather events to reduce the likelihood of planting field crops as farmers prefer to leave land fallow. Long-

term climatic averages play an important role in shaping crop choice decisions for instance, wetter conditions reduce the likelihood of leaving land fallow.

Results from our crop choice simulations indicate that farmers are likely to adjust their cropping patterns in response to evolving climatic and market conditions. Under the climate-change-only scenario, farmers are predicted to move away from soybean, wheat, and rapeseed and shift towards sunflower, and maize. When we incorporate yield effects, maize's initial gain reverses (shares decline), while wheat's initial decline reverses (shares increase). Allowing prices to adjust to yield-driven supply changes attenuates the maize decline. Overall, we find that farmers move away from soybean and maize towards the more resilient wheat and sunflower under climate change.

This paper proceeds as follows. Section 1.2 provides a background of the study area. Section 1.3 describes the theoretical and empirical framework behind the yield-weather and crop choice model. Section 1.4 outlines the data used, and Section 1.5 presents the results from the yield-weather, crop choice model and the simulations. Section 1.6 discusses the way forward and section 1.7 concludes.

1.2 Study Area

Agriculture is at the heart of Serbian economy. The sector accounts for 12% of the GDP and employs approximately 21% of the labor force (International Trade Administration, 2024). Agriculture is mostly prevalent in the Vojvodina region. Commonly planted crops in the region include maize, soybean, sugar beet, sunflower, rapeseed, and wheat. These crops make up a significant share of Serbia's agricultural exports especially to the European Union and the US generating revenues of approximately $5.3 billion in 2016.

Over the last two decades, however, Serbia's agricultural sector has suffered tremendous losses due to climate change. An increase in the frequency of extreme weather events, including droughts, floods, and frost has hurt crop yields and agricultural production (FAO, 2023). In 2022 alone, the persistent drought lasting over 4 months reduced crop yields by 20-30%, incurring economic losses reaching a billion dollars (Maslac, 2022).

Given the high risks that farmers are facing, there might be measures employed by farmers to

mitigate the impacts of climate change. Farmers might have adapted their crop choices to reflect the changing weather conditions. However, little research has been done to understand the impacts that this crop switching can have on farmers' welfare and overall economic output of the agricultural sector. Research evaluating climate change impacts has traditionally focused on a single crop or a smaller study region. This paper investigates how farmers' crop choices adjust under climate change utilizing field-level data across all of Serbia and includes the six major field crops planted across Serbia. Estimating the welfare implications of these adaptations offers valuable insights into the agricultural sector's future potential and can inform effective climate change policy in Serbia.

1.3 Conceptual Framework

Extreme temperatures and erratic rainfall patterns affect yields for all crops. However, the impact varies across crops depending on their comparative advantage. Adjusting crop choices allows producers to partially mitigate the negative consequences of climate change. Our crop choice model allows us to identify the key variables that determine farmers' crop choices. Through our crop choice model, we determine the role that short and long-term weather play in shaping farmers' cropping decisions. Moreover, we estimate how market conditions that shape farmers' expectations of profitability impact crop choices. The conceptual framework is provided in Figure 1.1.

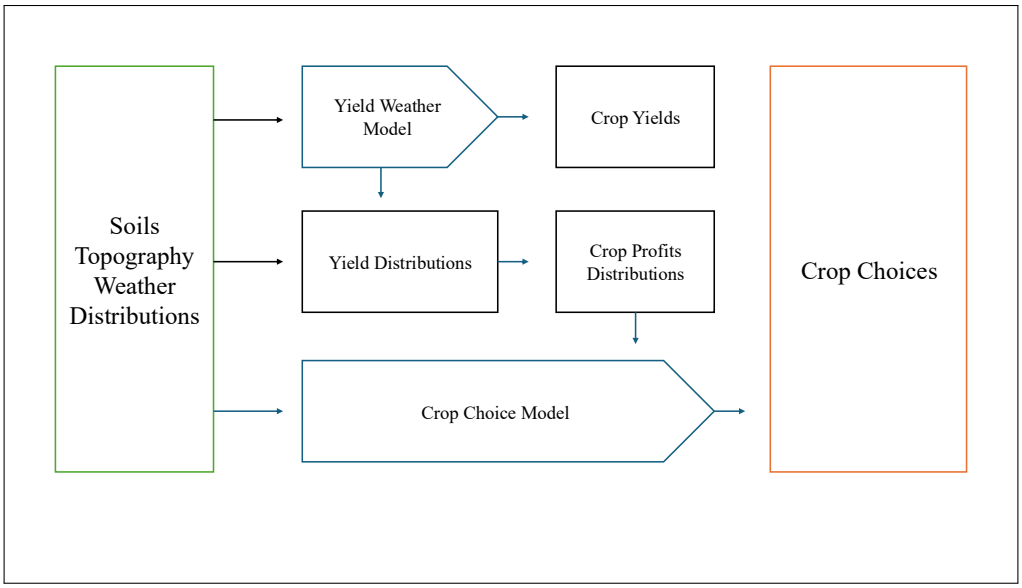

Figure 1.1 Conceptual Framework used in capturing climate change impact of crop choices. This figure is motivated by the conceptual framework employed in (Arora et al., 2020). However, it differs from their framework as we employ a yield model to derive profit measures – net returns from crops - and include those in a crop choice model.

In our first step, using a fixed effects panel estimation we estimate the following yield weather model with detrended crop-specific yields, Y_{it}^{dt}, for field i and year t ranging from 2017-2022 as dependent variables:

$$\ln\left(Y_{it}^{dt}\right) = \beta_0 + \sum_k \beta_k \,\text{TempExposureBin}_{k,it} + \gamma_1 \,\text{EarlySeasonSoilMoisture}_{it} + \gamma_2 \,\text{GrowingSoilMoisture}_{it} + \gamma_3 \,\text{HarvestingSoilMoisture}_{it} + \mu_i + \varepsilon_{it} \tag{1.1}$$

Equation (1.1) is estimated separately for each crop – maize, soybean, sunflower, rapeseed, and wheat where the weather variables are for the growing season. The growing season for spring crops (maize, soybean, and sunflower) is April to September (Kresovic et al., 2014) and for winter wheat and rapeseed is October to June (Dodig et al., 2017). Double cropping is highly uncommon in the Serbian context (Marković et al., 2022). $TempExposureBin_{k,it}$ represents the total hours field i in year t is exposed to temperatures within the $k-th$ temperature bin during the growing season. The exposure bins are constructed by interpolating temperatures at 15-minute intervals throughout each day using a sine function approximation between daily minimum and maximum

temperatures, following the methodology adopted by Ortiz-Bobea et. al. (2019). Soil moisture during the growing season is divided into distinct stages reflecting crop development periods. For spring crops, early season soil moisture covers April to May, the main growing season spans June to August, and harvesting season corresponds to September (Pandžić et al., 2020). For winter crops, early season moisture includes October to February , the main growing season extends from March to May, and harvesting occurs in June (Jeločnik et al., 2019).[1] These stage-specific soil moisture averages are used to capture differential impacts of soil moisture conditions throughout the crop growth cycle. Field fixed effects control for field characteristics that may impact yields, and standard errors are clustered at the more aggregated village-level.

We de-trend yields to remove the steady, long-term increase attributable to technological improvements, policy changes, and other factors. Given the short length of our panel, including a year trend fails to accurately capture these long-term improvements in yields. Therefore, we use an external national yield trend estimated from data spanning 2006–2023 (FAO, 2025a) and apply it uniformly across all crops. Although crop-specific trends may exist, due to data limitations we assume that broad technological improvements or policy changes affect all crops similarly. This approach allows us to isolate variations in crop yields that are solely attributable to weather changes.

Our yield weather regressions allow us to disaggregate temperature bins into beneficial and harmful temperatures for crop yields. It also allows us to more accurately estimate profits, which are particularly salient to producers. By quantifying the role that weather and market conditions play in determining crop choices, we can simulate how the choices adjust under plausibly exogenous shocks to these factors. A stylized model that embodies the decision-making process of a representative farmers is presented below.

For each parcel i, a grower chooses a crop type k in year t. We assume the grower is profit-maximizing and each parcel produces a single crop during a growing season (fallow ground, maize, wheat, soybean, sunflower, and rapeseed). Expectations of this year's profit for the given crop

[1]Wheat enters dormancy when temperatures approach 0–5°C (Johnson et al., 2009). During this phase, crop development is essentially paused, and water requirements are minimal. For this reason, we classify soil moisture during the dormancy period as part of "early season soil moisture.

k depend on past profits, $\Pi_{k,t-1}$, previous growing season's weather variables, $W_{i,t-1}$, long-term moving climatic averages, $V_{i,t-m:t-1}$, and other field-specific attributes, X_i.

Under these assumptions, a grower will choose to plant the crop on parcel, i, that yields the maximum profit. The outside option is $k = 0$, leaving the land fallow and its profits are normalized to 0. The grower's choice problem can be defined as

$$\Pi_{it} = \max_{k \in \{0,1,\ldots,K\}} \left(\Pi_1^*(\Pi_{1,t-1}, W_{i,t-1}, V_{i,t-m:t-1}, X_i), \ \ldots, \ \Pi_K^*(\Pi_{K,t-1}, W_{i,t-1}, V_{i,t-m:t-1}, X_i) \right) \quad (1.2)$$

The probability of choosing crop k at time t to plant on parcel i is then represented as

$$\rho_{ikt} = \Pr \left[\Pi_k^*(\Pi_{k,t-1}, W_{i,t-1}, V_{i,t-m:t-1}, X_i) \ > \ \Pi_j^*(\Pi_{j,t-1}, W_{i,t-1}, V_{i,t-m:t-1}, X_i), \ \forall j \neq k \right] \quad (1.3)$$

where ρ_{ikt} equals 1 if crop k is planted on parcel i at time t and 0 if any other crop is chosen.

Current period profits can be estimated as

$$\pi_{k,it} = \alpha \pi_{k,it-1} + \beta_k W'_{i,t-1} + \eta_k V'_{i,t-m:t-1} + \omega_k X'_i + \theta_k \text{ Year} + \tau_k + \varepsilon_{k,it} \quad (1.4)$$

where α represents the impact of previous season's profits. $W'_{i,t-1}$ consists of previous growing season's weather variables, including hours of exposure above heat stress and below the cold stress thresholds, and soil moisture anomalies. $V'_{i,t-m:t-1}$ consists of crop-specific moving climatic averages for temperatures and soil moisture during the growing season over a 29-year period.

Weather and climatic variables are assigned based on crops' growing season: spring crops are assigned weather from the spring growing season, while winter crops are assigned weather of the winter growing season. Due to collinearity between spring and winter season weather and climate variables, $W'_{i,t-1}$ incorporates extreme temperature metrics (heat and cold stress) from both seasons but includes only spring season soil moisture anomalies. Similarly, $V'_{i,t-m:t-1}$ includes moving averages solely for the spring season's temperature and soil moisture. Including all weather and climatic variables in the model leads to convergence issues, motivating the selective inclusion approach adopted in this study.

X'_i contains field characteristics including field size, elevation, soil quality, and access to irrigation. Year trends are included, a crop-specific fixed effect τ_k, and field-by-year random effects are also controlled for in the analysis.

The spatial and temporal variation that is present allow for the estimation of a panel conditional logit model, which accounts for repeated choices at different periods of time.If $\varepsilon_{k,it}$, a random error term, is assumed to follow a type I extreme value distribution, then the probability of choosing the kth crop can be rewritten as

$$\rho_{ikt} = \frac{e^{\pi_{k,it}}}{\sum_{k=0}^{K} e^{\pi_{k,it}}} = \frac{e^{\pi_{k,it}}}{1 + \sum_{k=1}^{K} e^{\pi_{k,it}}} \tag{1.5}$$

where the parameters can be estimated by maximum simulated likelihood. Controlling for field by year random effects relaxes the assumption of independence of irrelevant alternatives (IIA) to a degree by allowing correlation between choices over time (McFadden and Train, 2000). This is a significant benefit as the IIA assumption is unrealistic in the context of repeated choices of field crops over time. We employ a panel conditional logit framework also provides us the opportunity to simulate the effects of climate change. For inference, we also cluster the standard errors at the village level.

There are some potential identification concerns regarding our analysis. Weather can be endogenous to crop choices particularly if it is influenced by the actions of an individual farmer. This concern is more relevant for soil moisture as certain crops can influence the amount of moisture that is retained in the soil (Mendis et al., 2022). We use lagged growing season weather variables which are unaffected by farmers' future crop choices. Additionally, our soil moisture estimates are derived from the SWAT+ model at a more aggregated subbasin-level. Soil moisture the aggregated subbasin level is largely determined by the interaction of temperature and hydrological components and is unlikely to be influenced by individual farmer behavior.

Crop choices may be influenced by unobserved economic and political factors. We explicitly control for field characteristics including size, elevation, and access to irrigation, that can play an important role in shaping crop choices. We include a linear time trend to control for any unobserved factors that affect weather and crop choices simultaneously. Finally, we include field by year random effects to account for any field level effects that are correlated with weather.

We do not explicitly model crop rotations, although they can influence crop choice by linking current decisions to past planting and by affecting soil health, yields, and profitability. However, in

our dataset, there are no dominant or well-defined rotation patterns, as shown in Table 1.1 below. Additionally, we account for rotation-related effects indirectly by explicitly controlling for profits, which capture much of the agronomic and economic impact of rotations. We also run a specification that includes lagged crops (See Section A.3 table A.7).

	Maize	Wheat	Soybean	Sunflower	Oilseed	Fallow
Maize	0.37	0.25	0.15	0.23	0.00	0.00
Wheat	0.56	0.19	0.06	0.15	0.04	0.00
Soybean	0.50	0.18	0.28	0.03	0.00	0.00
Sunflower	0.33	0.62	0.01	0.04	0.00	0.00
Oilseed	0.35	0.50	0.04	0.07	0.05	0.00
Fallow	0.13	0.10	0.03	0.02	0.00	0.73

Table 1.1 Conditional Probability Matrix of Crop Transitions. This table shows the conditional probability matrix of crop transitions from 2016-2022. We drop all fields consistently classified as non-agricultural land (category 20) throughout 2016–2022, as well as fields that exited agriculture (land classified as 20 consecutively from 2020–2022). Observations where the crop planted was sugar beet or other crops are also excluded. For each current crop, we identify the probabilities of transitioning to all possible subsequent crops. Our results show that no dominant rotation exists in the data. In fact, farmers in Serbia have diverse cropping strategies.

Finally, it is important to note that the outside option in our crop choice model is leaving land fallow. We do not model the choice to move to a specialty crop or to exit agriculture. We drop all fields that are classified as non-agricultural or "other crops" as these alternatives are fundamentally different field crops choices. Specialty crops often involve long-term investments making it difficult to compare their profits directly to profits earned by field crops. Similarly, exiting agriculture may involve a lump-sum payments, which are not comparable with annual profits earned by field crops. Our model specifically focuses on capturing switching decisions between planting field crops and leaving land fallow in response to climate change and does not account for longer-term exit decisions We believe this limitation does not significantly affect our findings since only 0.02% of fields growing field crops were left fallow for three consecutive years during 2018–2022, indicating minimal permanent exit. Furthermore, under extreme drought conditions in 2017, 2021, and 2022, only 0.7% of fields were left fallow. This suggests that land abandonment due to drought or climate stress has historically been limited, supporting the assumption that permanent exit is not a major

factor within our study period. While recent demographic data indicate a 6% decrease in agricultural land between the 2018 and 2024 censuses (Agroberichten Buitenland, 2024), future research could incorporate more detailed scenarios of agricultural exit as demographic and economic transitions evolve.

1.4 Data

1.4.1 Yield data

We obtain pixel-level data on observed yields [2] from 2017-2022 for six crops, maize, soybean, sugar beet, sunflower, wheat and rapeseed, for Vojvodina region (Bisosense, 2024). Each pixel is 216.07m×216.07m and represents yields in tons per hectare. Since we want to model decision-making at the field-level, we convert the pixel to field-level yield data (details are provided in Supplementary information A.1.1).

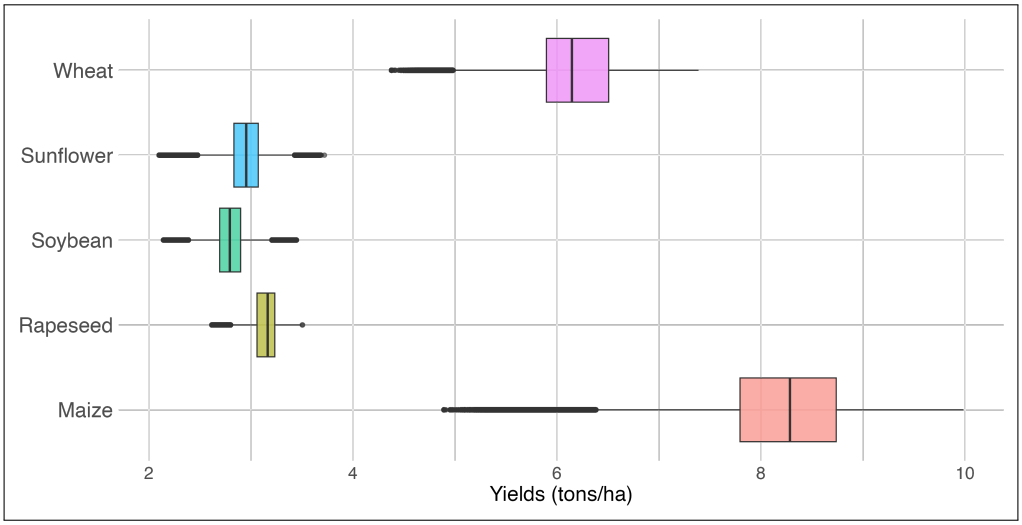

Figure 1.2 Crop Yields Distributions (2017-2022). This figure shows the variation is yields within and across crops. We pool every field's annual yield observation from 2017 through 2022, so that both cross sectional (field to field) and temporal (year to year) variation are shown. Maize and wheat tend to have the highest variability in yields. Soybean, sunflower, and rapeseed tend to have tightly clustered yields.

[2] Fields with no yield data are not considered in the analysis. Most fields having missing yield data are classified as non-agricultural land.

1.4.2 Crop data

Pixel-level annual planting data for six major crops is obtained from Landsat and Sentinel-2 images for 2018-2022 with an accuracy of over 90% for each year (Živaljević et al., 2024). Each pixel of 10 m x 10 m dimensions is categorized into maize, wheat, soybean, sugar beet, sunflower, rapeseed, other crops – a single crop category that consists of orchards, vegetables, alfalfa or clover - or non-agricultural land. While the pixels are located across all of Serbia, 95% of the pixels in our analysis are in Vojvodina as agriculture is mainly present in this region.

Pixel-level data on crops is converted into field-level data using a cadastral map of field boundaries in Serbia. Our decision to move from pixel to field-level data is justified as planting decisions are often made at the field-level. For classifying the field into one of the crop categories, we use the crop that is planted on the majority of pixels within the field's boundaries. However, in doing so, we might be introducing some crop-specific bias, particularly affecting crops traditionally planted as secondary crops. To ensure that such crop-specific bias is not present in our analysis, we compare the percentage share of crops covered under pixel vs field-level data. Details on data construction and the test for crop-specific bias can be found in the supplementary text (A.1.2).

We drop land classified as non-agricultural land is also removed from the dataset (37% of fields get dropped). Fields classified as "other crops" and sugar beet from our final dataset. Other crops are dropped due to their heterogenous nature as high-value crops are lumped together with low-value crops (29% of fields get dropped). Sugar beet is excluded because profit data for this crop are unavailable; however, since it is planted on 1.6% of fields, its removal is unlikely to affect results significantly. Additionally, fields presumed to have exited agriculture—identified as those left fallow for three consecutive years (approximately 0.02% of the sample)—are excluded. The final dataset is an unbalanced panel of 1473701 fields. Year-wise field-specific shares are presented in the supplementary materials.

1.4.3 Temperature

Data on daily maximum and minimum temperatures in degree Celsius are obtained from E-OBS from 1988-2022 (Cornes et al., 2018). This high-resolution (0.1°) gridded dataset is interpolated

from meteorological observations from weather. The minimum temperature reported from 1988-2022 is -34°C and the maximum temperature reported is 45°C. August is the hottest month in Serbia and January is the coldest month.

For the yield weather model, we use daily maximum and minimum temperatures from 2017 onwards to obtain total hours obtained in 3°C bins. To estimate hours of exposure, we replicate sine function approximation method adopted by Ortiz-Bobea et al. (2019) to convert daily minimum and maximum temperatures into 15-minute interval estimates. The number of 15-minute intervals within each temperature bin is counted for each month and then converted to hours. These monthly exposure hours are aggregated over the growing season to obtain total hours of exposure per bin. Finally, to reduce noise from sparse data, we aggregate bins with negligible exposure and combine 1°C bins into broader 3°C bins.

In our crop choice model, we include both short and long-term temperature variables that can influence farmers' crop choices. To capture the impact of fluctuations in recent temperatures, we include heat and cold stress variables. We rely on temperatures from the previous year's growing season because at the time farmers make their planting decisions, information about the current year's growing season is not yet available. Consequently, farmers base their expectations for the current year's weather on historical temperatures. We include variables on extreme temperature events in our crop choice model. We believe that including extreme temperatures is crucial as farmers experiencing extreme heat or cold temperatures in the previous season may switch to more tolerant crops. Crop-specific thresholds on extreme temperatures are identified from the yield-weather models. These thresholds are incorporated to create crop-specific heat and cold stress variables that represent the total number of hours crops are exposed to temperatures above the heat and below the cold thresholds during the previous growing season. Along with short-term temperature measures, we include 29-year moving historical averages of mean temperature to account for regional climatic differences influencing crop suitability. Details on the construction of temperature variables for the yield and crop choice model are presented in Supplementary text (A.1.3).

1.4.4 Soil Moisture

Data on monthly soil moisture is obtained from Soil and Water Assessment Tool-Plus (SWAT+), a semi-distributed, process-based hydrologic model, using daily data on precipitation, temperature, humidity, and solar radiation (Jalali et al., 2025). As soil moisture outputs from SWAT+ model are available at the aggregated subbasin level, these measures are spatially downscaled to the field level (Details on the construction of the variables are provided in the Supplementary text A.1.4).

In the yield model, monthly data are aggregated to annual averages using mean soil moisture over the growing period. Soil moisture during the current growing season enters the yield–weather model as the average across distinct phenological stages. In the crop choice model, we include both soil moisture anomalies and the 29-year moving historical average of growing season soil moisture. Soil moisture anomalies capture deviations from long-term moisture conditions (Copernicus European Drought Observatory, 2019). We construct a soil moisture anomaly indicator at the monthly level as

$$SMA_{m,t} = \frac{\text{Observed}_{m,t} - \overline{\text{Soil Moisture}}_m}{\sigma_m} \tag{1.6}$$

where $\overline{\text{Soil Moisture}}_m$ denotes the long-term average and σ_m is the standard deviation for month m, calculated over a baseline window (1988–$t-1$). The monthly averages are averaged across spring and winter growing season to obtain yearly soil moisture anomalies. The indicator takes both positive and negative values: positive values indicate wetter-than-normal conditions, while negative values indicate drier-than-normal conditions.

A potential limitation of this approach is that soil moisture anomalies are calculated at monthly level, however, the SMA indicator constructed by Copernicus European Drought Observatory relies on higher-frequency (daily or hourly) data. As a result, our indicator may underestimate the magnitude of extreme soil moisture conditions. Nevertheless, because this coarser resolution applies uniformly across both wet and dry years, the indicator remains suitable for capturing fluctuations in seasonal moisture availability.

1.4.5 Profits

Crop-specific profits are constructed using field-level data on observed yields from 2017 to 2022 and country-level crop prices (FAO, 2025b). For each field, revenue is calculated as the product of crop yield and price. To obtain annual crop-level revenue estimates, we aggregate field-level revenues using a weighted average, where each field's contribution is weighted by its area. This approach ensures that larger fields—which contribute more to total production—have proportionately greater influence in the overall revenue estimates. The revenues are then subtracted with costs of production data obtained from a survey of 728 for the period of 2015-2020 (BioSense Institute, 2022). Crop-specific costs of production include raw material costs for seed, fertilizers and pesticides, and machinery and labor costs for sowing, tillage, fertilizer and pesticide application, and harvest. As we utilize profits from the previous year in our crop choice model, we need profit data spanning from 2017 to 2021. However, since our survey data only extends through 2020, we use inflation-adjusted costs for 2021. Additionally, any missing cost values within the survey period are interpolated using the same approach.

1.4.6 Field Attributes

Data on soil quality for the subbasins in the Danube Water shed is obtained from Harmonized World Soil Database (Fischer et al., 2008) that contains data on worldwide different soil mapping types. Available water capacity is used to represent the soil quality – details are provided in supplementary text (A.1.5). Data on elevation are obtained from a digital elevation model (European Environment Agency, 2019). Field area is calculated using the field boundaries in the data.

To construct a variable on access to irrigation, we use pixel-level data on irrigation status of maize, soybean, and sugar beet from 2020-2022 (Radulović et al., 2023). The data on irrigation is obtained through visual detection of irrigation infrastructure from satellite images, supplemented with survey data of farmers' fields. Irrigation data is only available for the above-mentioned crops because these are among the most irrigated crops in Serbia, making up 41% of the total irrigated area among all irrigated field crops (Statistical Office of the Republic of Serbia, 2024).

We convert pixel-level irrigation data to field-level data using field boundaries. A field is

classified as irrigated if 50% more pixels within the field's boundary are irrigated. To create an indicator variable of irrigation access, we assume that if a field is irrigated in any year during the 2020-2022 period, it is considered to have access to irrigation for all the years included in our analysis. This results in 1.1% of the fields having access to irrigation in the sample [3].

1.4.7 Simulations of Climate Change Impact on Yields and Crop Choices

For our climate change scenarios, we obtain EURO-CORDEX data on bias-adjusted regional climate simulations (Dosio, 2016). This dataset includes downscaled Global Climate Model (GCM)-Regional Climate Model (RCM) simulations that provide daily time series future weather projections from 1981-2100 for CMIP5 RCP 4.5 and 8.5. Five distinct climate models were run under both RCP scenarios – details are provided in Table 1.2 below.

Institute	**RCM**	**Driving GCM**
CLMcom	CCLM4-8-17	CNRM-CERFACS-CNRM-CM5
		ICHEC-EC-EARTH
		MPI-M-MPI-ESM-LR
IPSL_INERIS	WRF331F	IPSL-IPSL-CM5A-MR
KNMI	RACMO22E	ICHEC-EC-EARTH

Table 1.2 Bias-adjusted GCM-RCMs Utilized in SWAT+ model Simulations. Source: (Dosio, 2016)

We utilize future daily temperature projections for RCP 4.5 to construct ensemble mean temperature data across five climate models. Similarly, simulations outputs for the five distinct climate models obtained from the SWAT+ model were used to obtain ensemble mean of soil moisture data. Overall, future projections show an increase in mean temperatures and a decrease in precipitation compared to the observed, historic (1991-2020) weather data.

We investigate the impact of climate change on yields and crop choices using the future climate data in the mid-century: 2040 - 2070. For the yield model, our simulations allow us to predict

[3]While irrigation data is available only for three out of the six crops in our analysis, through the construction of our access to irrigation variable, we can observe irrigation for wheat, sunflower and rapeseed in our analysis. As a field that is irrigated in at least one year from 2020-2022 is considered to have access to irrigation for all years in our sample, this construction allows us to observe irrigation for wheat, sunflower and rapeseed. Among fields with access to irrigation, 43% have maize, 29% have soybean, 6% have sugar beet, 15% have wheat, 5% have sunflower, and 1% have rapeseed planted on them.

field-level crop yields during 2040-2070 period conditional on field characteristics and static year trends. In the crop choice simulations, we update the short and long-term weather variables with future weather projections. Heat stress, extreme cold and soil moisture variables for the previous growing season are updated using the future data. 29-year moving historical averages are also updated accordingly. We also incorporate the effects of climate-induced changes in yields and prices. First, we include a scenario under which only simulated yields are utilized to construct future crop-specific profits. Predicted field-level yields are multiplied by baseline crop prices to obtain field-level revenues, which are then aggregated to annual, crop-level revenues using area-weighted averages. Finally, baseline production costs are subtracted from these projected revenues to yield future profits. Assuming baseline prices under climate change is a strong assumption. To relax the assumption of constant prices, we run an additional scenario in which crop prices adjust to reflect yield shocks. Using an instrumental variables approach (details can be found in A.1.6), we estimate that a 1% decrease in yields increases crop prices by 0.42%. This elasticity is then applied to adjust future prices based on deviations in simulated yields from baseline (2017-2022) average yields. Incorporating this simulation allows us to construct profit projections that account for both yield and price responses to climate change.

In our simulations, we only adjust weather, climate, and profit variables to reflect projected climate change, while holding fixed year trends, production costs, and other factors capturing technological and broader economic conditions at their baseline levels. This approach isolates the effect of climate by attributing differences between the baseline and simulated periods solely to climate-driven changes (Arora et al., 2020). Accordingly, our projected yields and crop choices are not unconditional forecasts of the future; rather, they indicate how yields and cropping decisions respond to changing climatic conditions, holding other determinants constant.

1.5 Results

1.5.1 Yield Weather Model Results

The results from our yield weather models are provided in Table 1.3 below - full regression results can be found in Supplementary text (A.3. Table A.4 & Table A.5). Our yield-weather

models reveal that extreme weather thresholds vary tremendously across crops. Yields for spring crops tend to start declining at temperatures lower than 4°C and temperatures above 34°C. For instance, an additional hour of exposure to temperatures above 34°C will decline yields by 0.2% for maize relative to base category of 16 to 19°C. Sunflower exhibits higher heat tolerance, as yields do not significantly decline until temperatures exceed 40°C (Debaeke et al., 2017).

Yields for winter wheat and rapeseed tend to decline at temperatures above 28°C. Specifically, an additional hour of exposure above 28°C reduces wheat yields by about 0.2%. The lower temperature thresholds for winter crops show unusual patterns; for instance, wheat yields do not decline until temperatures drop as low as -14°C. We suspect this result is due to the low number of exposure hours in the temperature bins below freezing.

	Maize	**Soybean**	**Sunflower**	**Wheat**	**Rapeseed**
SPRING CROPS					
Cold Stress (< 4°C)	-0.0006**	-0.002***	-0.0008***	–	
Heat Stress (> 34°C)	-0.003***	-0.015***	0.002***	–	–
Early Season Soil Moisture (Apr–May)	1.62e-05	-0.00036***	0.00046***	–	–
Growing Soil Moisture (June–Aug)	0.001***	0.0013***	0.00027**	–	–
Harvesting Soil Moisture (September)	-0.002***	-0.003***	-0.0006***	–	–
WINTER CROPS					
Cold Stress (< −5°C)	–	–	–	0.0008***	0.0012***
Heat Stress (> 28°C)	–	–	–	-0.0007***	-0.0004***
Early Season Soil Moisture (Oct–Feb)	–	–	–	-0.0013***	-0.0003***
Growing Soil Moisture (March–May)	–	–	–	0.0005***	0.0005***
Harvesting Soil Moisture (June)	–	–	–	0.0002***	4.44e-05

Table 1.3 Marginal Effects of Temperature and Soil Moisture on Crop Yields. The table present the marginal effects of temperature bins and soil moisture for different growth stages on crop-specific yields. The results are from a two-way fixed effects estimation that controls for field fixed effects. Standard errors are clustered at village-level. Significance and confidence intervals are obtained from bootstrapping with 9,999 replications. The results show the thresholds of extreme weather vary significantly across crops.

Overall, our findings on extreme temperature thresholds align with previous literature. The upper temperature threshold for spring crops generally falls between 30°C and 35°C. Maize yields tend to decline at temperatures around 29–30°C, while soybeans are typically more heat-tolerant, with yield declines occurring above 32°C (Miao et al., 2016; Ortiz-Bobea et al., 2019). Interestingly,

we find that maize and soybean yields decline at similar temperature ranges in our data. This can be explained by the differences in crop varieties as Serbian farmers mainly use domestic cultivars (Agroberichten Buitenland, 2020). Our results also remain robust to different specifications (1-degree and 2-degree temperature bins). Notably, we find soybean to be much more responsive to temperature changes with significantly larger coefficients on both, beneficial and harmful bins.

Results for winter crops are slightly different from the existing literature. While winter wheat yields start declining at temperatures above 25°C (Ortiz-Bobea et al., 2019), we find wheat to be more heat tolerant as evidence points that Serbian wheat exhibits higher resilience under climate stressors (Mirosavljević et al., 2024).

Soil moisture exerts a stronger influence on water-intensive crops such as maize and soybean, as reflected in the larger marginal effects relative to less water-dependent crops like wheat and sunflower. As expected, excessive soil moisture during planting and harvesting stages is detrimental for crop yields. However, it is surprising to observe a positive impact of early season soil moisture on sunflower yields. Similarly, late season soil moisture shows a positive effect for wheat and rapeseed. This aligns with evidence indicating that successful seedling establishment in sunflower depends on adequate soil moisture during planting (Sghaier et al., 2023). On the other hand, soil moisture during the grain-filling stages is critical for maximizing wheat and rapeseed yields (Sokoto and Singh, 2013).

Our yield model demonstrates good prediction accuracy, significantly improving over a baseline model with only year trends and fixed effects – as observed by the reduction in root mean squared error (RMSE) (Figure 1.3). However, the degree of improvement varies across crops. Soybean shows the highest increase in prediction accuracy, followed by rapeseed and maize. Our yield model's performance aligns with existing literature, showing slightly improved accuracy. For example, Ortiz-Bobea et al. (2019) report a maximum RMSE reduction of around 20%, which is comparable to or slightly lower than our results. The relatively low RMSE for sunflower implies that weather does not explain variation in sunflower yields as much as it does for other crops. This is consistent with historical data from 2006–2023 (FAO, 2025), where sunflower yields remained

relatively stable despite multiple drought years. The lower accuracy could be due to either (1) sunflower's inherent resilience to extreme weather which is confirmed by historical yield data where national averages for sunflower yield only decline by 14% in drought years as compared to 40% reduction in crops like maize or (2) other unmodeled factors, such as pests or diseases, influencing yields. If the latter is true and these factors worsen with climate change, our model may underestimate climate impacts on sunflower yields. To resolve this, we plan to include simulations with shocks to sunflower prices and production costs to capture these factors.

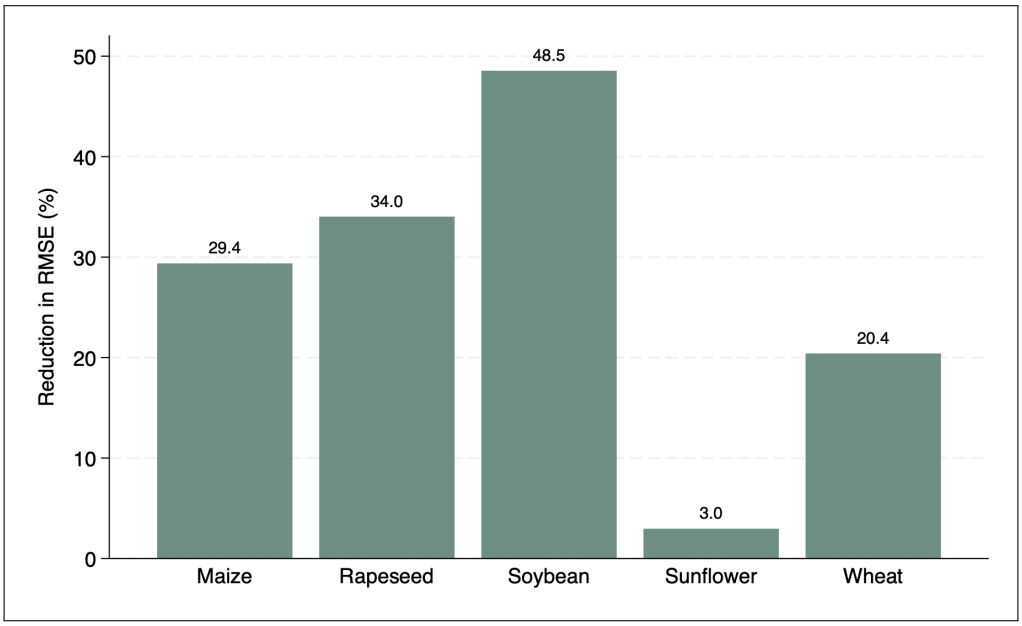

Figure 1.3 Yield Model Prediction Accuracy Across Different Crops. The figure displays the reduction in root mean squared error (RMSE) achieved by our yield model for different crops relative to a baseline model containing only year trends and fixed effects. We assess out-of-sample prediction accuracy using 10-fold cross-validation at the field level, where 10% of fields (all years) are held out in each fold. The model is trained on the remaining data, and predictions are made for the held-out fields. The RMSE is calculated for each fold and averaged to obtain an overall out-of-sample RMSE. Soybean shows the highest improvement in predictive accuracy with nearly 49% reduction in RMSE, followed by rapeseed and maize with reductions of approximately 34% and 29%, respectively. Wheat exhibits moderate improvement, while sunflower shows the least reduction, indicating that weather variables explain less of its yield variation.

The results from the yield-weather regressions are then integrated in our crop choice model by defining heat and cold stress variables using identified temperature thresholds. For spring crops heat stress occurs when temperature exceeds 34°C and cold stress occurs at temperatures below

4°C during the growing season. For winter crops, heat stress occurs at temperatures above 28°C and cold stress occurs at temperatures below -5°C.

1.5.2 Climate Change Impact on Yields

To evaluate the implications of climate change on crop yields, we replace climatic variables in our baseline yield-weather regressions with future weather to predict field-level yields. The results are presented in Figure 1.4 below.

Our results from the yield-weather simulations provide some interesting insights. We find that climate change impacts on yields vary significantly across crops. Maize remains the most affected crop with consistent decline in its yields across all simulation periods. In most blocks, the confidence intervals are below zero – indicating meaningful decline in yields. Soybean is particularly interesting. The crop's yields are projected to decline by almost 20% in 2040-2045 simulation period, then increase by almost 20% from the baseline in 2045-2050 simulation period. The changes are more moderate post 2050-2055 simulation blocks, and the prediction is also with higher uncertainty.

The differences in the response of maize and soybean yields to climate change are particularly fascinating. The initial gains in soybean yields can be explained by the results from the yield-weather model and the projected climate conditions. The period from 2040-2055 is projected to have moderate warming (see Supplementary Text A.2, Table A.3), with a shift away from colder temperatures and an increase in hours of exposure to temperatures ranging from 7-25°C. Since soybean yields are highly responsive to these temperatures (as observed from the large regression coefficients) – these changes are likely to positively impact yields in the early future periods. In contrast, for maize, the benefits from increased exposure to beneficial temperature bins are much smaller and are outweighed by losses due to greater exposure to harmful high temperatures. Additionally, differential responses to soil moisture during key growth stages also contribute to the divergence in yield outcomes between the two crops.

Sunflower yield changes are relatively stable with changes relatively between -1% to +4% – pointing to the crop's resilience. There is also uncertainty in prediction. Changes in wheat yields

are also relatively modest ranging between 0-5%.

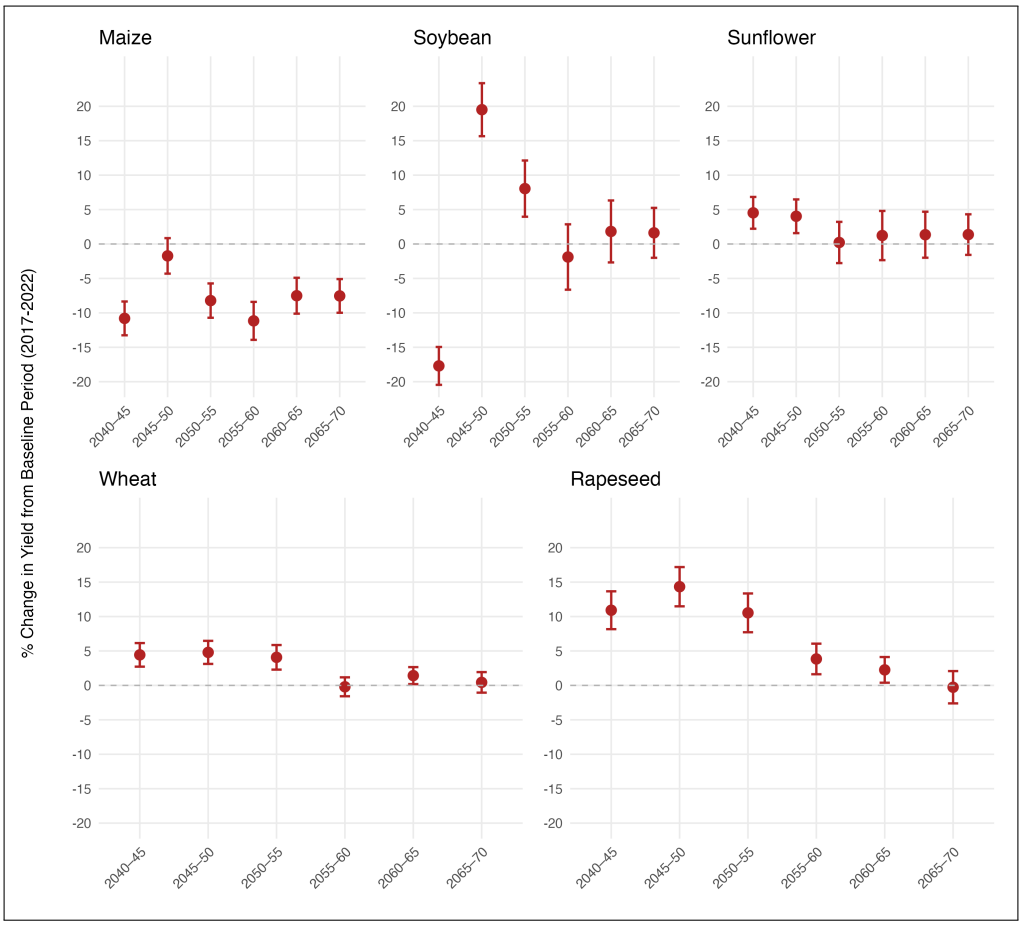

Figure 1.4 Predicted Change in Crop-specific Yields (%) Relative to the Base Period (2017-2022). This figure shows the changes in average yields for each simulation block relative to the base period. Vertical bars represent confidence intervals from the delta method. For each field, baseline yields are predicted with observed weather, and future yields are predicted by replacing weather covariates with the block-specific future weather while holding the non-weather trend fixed at the baseline average year. Uncertainty from estimation of regression parameters is represented through the confidence intervals. We only include statistical uncertainty in our predictions. Uncertainty from climate models is not included as we utilize projections from an ensemble mean across all climatic models. Overall, we find maize shows persistent declines, soybean exhibits mid-century gains, wheat effects are modest, and sunflower changes are small and often indistinguishable from zero.

Results for the yield responses under climate change are drastically different from what is found in the literature particularly, for soybean and winter wheat. Studies focused on the US find soybean and wheat yields to decline significantly due to warmer and drier conditions predicted under climate change (Yu et al., 2021; Tack et al., 2015). Moreover, yield projections in the literature often exhibit

less uncertainty, with tighter confidence intervals, as shown by Ortiz-Bobea et al. (2019).

Our results in fact align closely with the literature focusing on Serbia. Climate change impact assessments in Serbia project increases in soybean and wheat yields. For instance, soybean yields are predicted to increase by 20-50% by mid-century in many locations (Tovjanin et al., 2015). Likewise, wheat yields are predicted to increase under climate change (Mihailovic et al., 2015).

Lastly, the larger uncertainty in our yield projects stems from the fact that our analysis is conducted at the field-level. This approach captures spatial heterogeneity in climate change impacts across individual fields, revealing substantial variation in both the direction and magnitude of projected yield changes. Such heterogeneity is typically masked in aggregated, regional- or country-level projections, which leads to tighter confidence intervals. A further source of uncertainty in our results may arise from the relatively short length of our historical panel, which can amplify variability when projecting several decades into the future. Extending the panel would likely smooth some of these variations and further refine the projections.

1.5.3 Crop Choice Model Results

Results from the crop choice model are presented in Table 1.4 below - full results can be found in the Supplementary text (A.3 Table A.6). We report the coefficients from the conditional logit model, as average partial effects are generally less informative in the context of climate change analysis. The estimated log-odds ratios provide clear insights into both the direction and statistical significance of the effects. Complemented by our simulations, these results illustrate how various weather variables interact and jointly influence crop choice decisions. We are currently computing average partial effects for field-level attributes; however, given the model's high computational complexity, these results are still in progress. All results are presented relative to the outside option of leaving the land fallow.

Lagged crop-specific profits have a positive impact on the likelihood of planting that crop. This means that if the profits realized from planting a crop in the previous year increase, the likelihood of choosing that crop in the current year increases.

Turning to field-specific attributes, we find that an increase in heat stress days during the

spring growing season reduces the likelihood of planting all crops. In other words, as days with temperatures above 34°C during the spring growing season increase, farmers are more likely to leave land fallow rather than risk planting. Interestingly, heat stress days during the winter growing season increase the likelihood of planting both spring and winter wheat relative to leaving land fallow. This result can be explained by the timing of exposure to temperatures greater than 28°C, which primarily occur from June onward, coinciding with the end of the winter crop season. As winter crops mature from October to June, heat stress is experienced mainly around harvest. Warmer end-of-season conditions can promote timely maturation and facilitate harvest (de Perez et al., 2023). Moreover, exposure to temperature exceeding 28°C in early growing season is ideal for crop growth thereby, explaining the increase in the probability of planting spring crops (Minoli et al., 2022).

An increase in cold-stress days during the spring growing season reduces the likelihood of planting spring crops—especially maize and soybean—relative to leaving land fallow. In contrast, the likelihood of planting wheat and sunflower relative to leaving land fallow increases, although the estimated coefficients are not statistically significant. During the winter growing season, more days with temperatures below -5°C reduce the likelihood of planting all crops (except for rapeseed), however, the effect is only statistically significant for sunflower and wheat. This is intuitive, as Serbia's spring and winter growing seasons overlap: colder winter days can delay spring planting through frost and other constraints.

An increase in deviations from average soil moisture —indicating either unusually dry or unusually wet conditions— reduces the probability of planting maize, soybean, and rapeseed. This likely reflects these crops' sensitivity to both moisture deficits (which hinder germination and early growth) and excess water (which causes waterlogging and delays field operations). Consistent with this, evidence suggests rapeseed production is highly sensitive to extremely dry or wet conditions (Kandel and Knodel, 2021). By contrast, soil-moisture anomalies are associated with a higher likelihood of planting sunflower and wheat relative to leaving land fallow; however, these coefficients are not statistically significant. The statistically insignificant coefficients for

sunflower and wheat indicate that planting decisions for these crops are relatively insensitive to short-term deviations in soil moisture, consistent with their greater tolerance to moderate variations in water availability.

Long-term climatic trends in spring temperatures play a significant role in shaping crop choices. Warmer historic spring conditions increase the likelihood of planting winter wheat; rather than leaving land fallow, farmers tend to switch to winter wheat under milder spring climates. Similarly, the probability of planting sunflower rises with higher historic spring temperatures, reflecting the crop's resilience to warmer conditions. The positive coefficient for maize is also expected, as it is traditionally cultivated in Serbia's warmer regions.

Our results for long-term trends in spring soil moisture are consistent with our expectations: wetter spring conditions raise the probability of planting maize and soybean relative to leaving land fallow, reflecting their water-intensive nature. In contrast, higher long-term soil moisture reduces the likelihood of planting rapeseed, suggesting that this crop is more prevalent in less wet regions of Serbia.

Variable	**Conditional Logit**				
Lagged Profits (Inflated)			9.35e-06***		
			(2.35e-06)		
Crop-Specific Results	Maize	Soybean	Sunflower	Wheat	Rapeseed
Spring Season Heat Stress	-0.0015**	-0.0023***	-0.0057***	-0.0014**	-0.00046
	(0.0005)	(0.0007)	(0.0009)	(0.0006)	(0.0016)
Winter Season Heat Stress	0.0021**	0.0069***	0.0081***	0.0041***	-0.00028
	(0.001)	(0.001)	(0.0009)	(0.0008)	(0.0012)
Spring Season Cold Stress	-0.0079***	-0.0126***	0.014	0.0034	-0.0076
	(0.0029)	(0.0041)	(0.0031)	(0.0027)	(0.0048)
Winter Season Cold Stress	-0.0015	-0.0014	-0.005***	-0.0021**	0.001
	(0.0009)	(0.0013)	(0.0011)	(0.001)	(0.0019)
29-yr Moving Avg Spring Temp	1.37***	-1.8***	2.41***	1.28***	-0.53
	(0.18)	(0.31)	(0.23)	(0.20)	(0.34)
Spring Season Soil Moisture Anomalies	-0.30***	-0.69***	0.17	0.022	-0.45***
	(0.10)	(0.13)	(0.11)	(0.10)	(0.17)
29-yr Moving Avg Spring Soil Moisture	0.0042*	0.016***	-0.00065	0.0017	-0.011**
	(0.0022)	(0.0023)	(0.002)	(0.20)	(0.005)

Table 1.4 Conditional Logit Results by Crop.

Baseline option is leaving land fallow. All coefficients are relative to land left fallow.
Coefficients on field attributes and crop-specific coefficients are not included in the Table.
Robust (clustered by municipality) standard errors are in parentheses.
*** $p < 0.01$, ** $p < 0.05$, * $p < 0.1$.

To evaluate the predictive performance of the crop choice model, we implement a five-fold cross-validation procedure that randomly partitions the data into training subsets (70%) and test subsets (30%) by field. In each iteration, the model is re-estimated on the training subset and used to predict crop choice probabilities for the test sample. The predicted and observed crop shares are then aggregated across years for each alternative in the test sample. We find an average RMSE of 0.005 and a mean absolute error (MAE) of 0.004, indicating that the model predicts aggregate crop shares with high degree of precision. The small magnitude of these errors suggests that the estimated model captures most of the systematic variation in observed crop choice patterns across years and alternatives.

Our robustness test that includes previous season's crop choices (see Section A.3, Table A.7) shows that most of the estimated coefficients remain stable. The sign on spring heat stress changes

for some crops, reflecting that once crop persistence is controlled for, the model captures short-run rotational effects rather than broader adaptive responses. Because the baseline specification already distinguishes short-term temperature shocks from long-run climatic conditions, it provides the more appropriate framework for simulating future adaptation.

1.5.4 Climate Change Impact on Crop Choices

To evaluate the implications of climate change on crop choice, we perform three simulations. (1) In the Climate-Only Scenario, only the weather and climate variables in the crop choice model are updated to reflect future projections, keeping all other factors constant. (2) In the Climate + Yield Scenario, we also update profits using simulated field-level yields, calculated by multiplying future yields by baseline crop prices and subtracting baseline costs. (3) In the Climate + Yield and Market Adjustment Scenario, we incorporate both simulated yields and the corresponding price adjustments that arise from yield changes. Profits are recalculated using these simulated yields and prices, with costs held at baseline levels.

The results from the Climate-Only scenario are presented in Figure 1.5. The results reveal interesting patterns in crop substitution. Under changing climate – warmer and drier conditions – farmers are projected to reduce the cultivation of spring soybean and winter crops such as wheat and rapeseed.

The sharp decline in soybean area is primarily driven by the substantial increase in extreme heat days during the spring season. Days with temperatures exceeding 34°C are projected to rise by nearly 70% by mid-century, contributing to significant shifts away from soybean, which is highly sensitive to heat stress. This is consistent with soybean exhibiting the largest negative coefficient among all crops in the model. The decline in soybean can also be attributed to increasingly dry conditions, reflected in more frequent negative soil moisture anomalies (indicating drier-than-normal periods) and an estimated 11% reduction in long-term soil moisture. Winter wheat and rapeseed experience comparatively smaller declines. For wheat, this reduction is primarily driven by the increase in extreme temperature events, while for rapeseed, it also reflects the impact of drier future conditions.

Under this scenario, farmers are also projected to shift toward sunflower and maize. The substantial increase in sunflower's share is primarily due to its tolerance to heat and drought conditions. Although sunflower is negatively affected by the rise in spring heat stress days, the overall expansion is largely driven by its strong positive response to long-term spring temperatures. This suggests that as average temperatures rise, farmers are increasingly inclined to plant sunflower. Maize also shows a significant increase in its share. The contrasting responses of soybean and maize can be explained by the opposite signs of their coefficients on long-term spring temperatures. The probability of planting maize rises with higher long-term temperatures, and with an expected 4% increase in average spring temperatures by mid-century, maize becomes a more favorable crop choice.

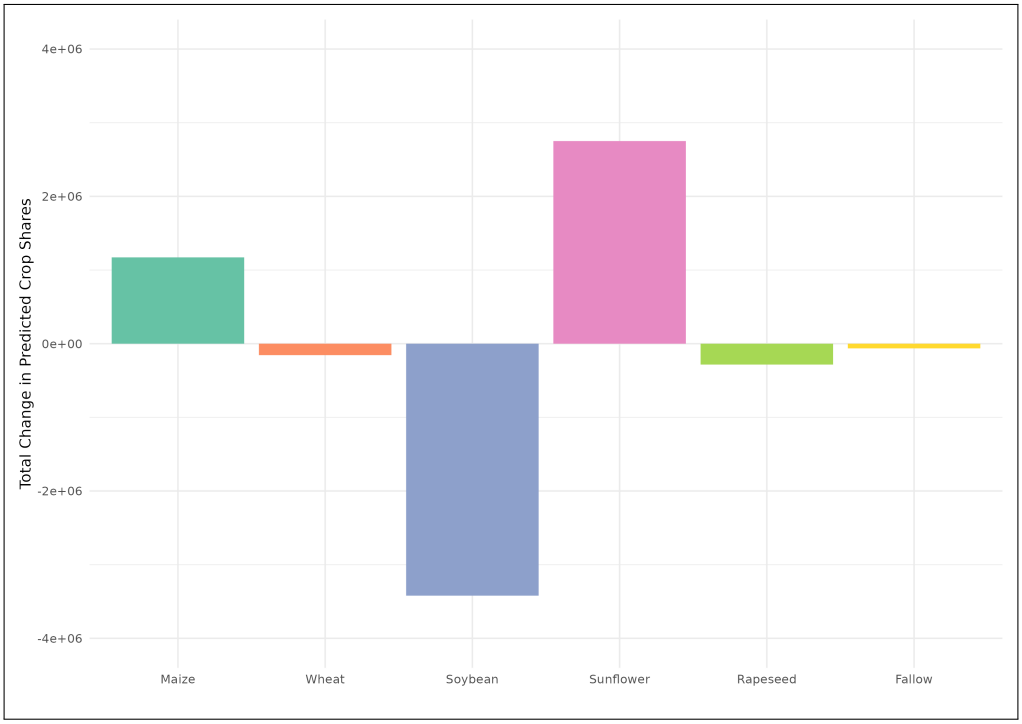

Figure 1.5 Change in Predicted Crop Shares under Climate-Only Scenario from 2040-2070 relative to Baseline (2018-2022). This figures shows projected changes in crop shares under climate change. Baseline crop shares are estimated using a crop choice model, and future shares are recalculated using projected weather and climate variables. Results indicate that farmers are likely to shift away from heat-sensitive crops such as soybean and adopt more resilient crops like sunflower and maize.

Farmers' crop choices are influenced not only by climatic conditions but also by expected

profitability, which itself can be altered by climate change. Figure 1.6 presents the results from the Climate + Yield scenario, in which profits are adjusted only for changes in yields, while prices are held constant at their baseline values. Comparing these results with the Climate-Only scenario (Figure 1.5) reveals several key differences: (1) maize shares decline; (2) wheat shares increase; and (3) the rise in sunflower's share is even greater than under the Climate-Only scenario.

These findings are consistent with expectations. The yield simulations indicate that maize yields are projected to decline substantially under climate change. With prices fixed, this decline directly reduces maize profitability, prompting farmers to shift away from maize. The increase in wheat's share, relative to its decline in the Climate-Only scenario, is also intuitive—wheat yields remain relatively stable under future climatic conditions, making it a more attractive option for farmers. Similarly, the larger increase in sunflower's share is primarily due to the crop's stable yields under climate change, reinforcing its position as a resilient choice in warmer and drier conditions.

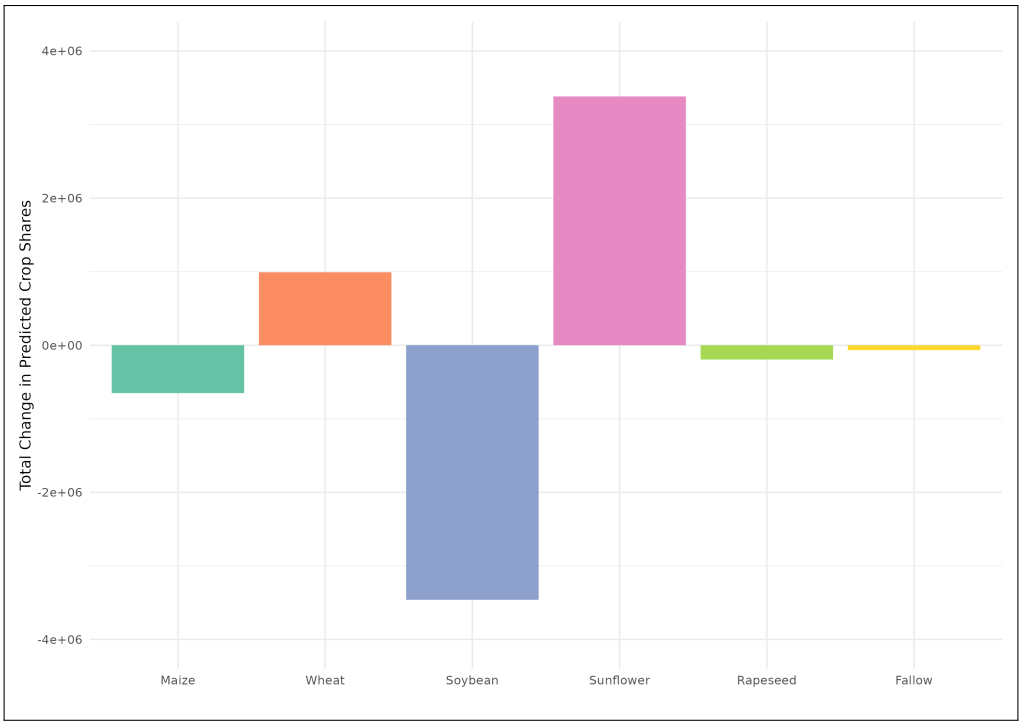

Figure 1.6 Change in Predicted Crop Shares under Climate + Yield Scenario from 2040-2070 relative to Baseline (2018-2022). This figure shows projected changes in crop shares when both climate and yields evolve over time. In this scenario, weather and climate variables are updated, and profits are replaced with predicted values based on field-level yields multiplied by baseline prices, net of baseline costs. Results indicate that under future climate and yield conditions, farmers are likely to shift away from maize, soybean, and rapeseed, and adopt more resilient crops such as sunflower and wheat.

The assumption that prices remain fixed under climate change is a strong one. Figure 1.7 presents the results from the simulation in which prices adjust in response to yield shocks. The results behave as expected: (1) the decline in maize is smaller, and (2) the increases in wheat and sunflower shares are also more moderate.

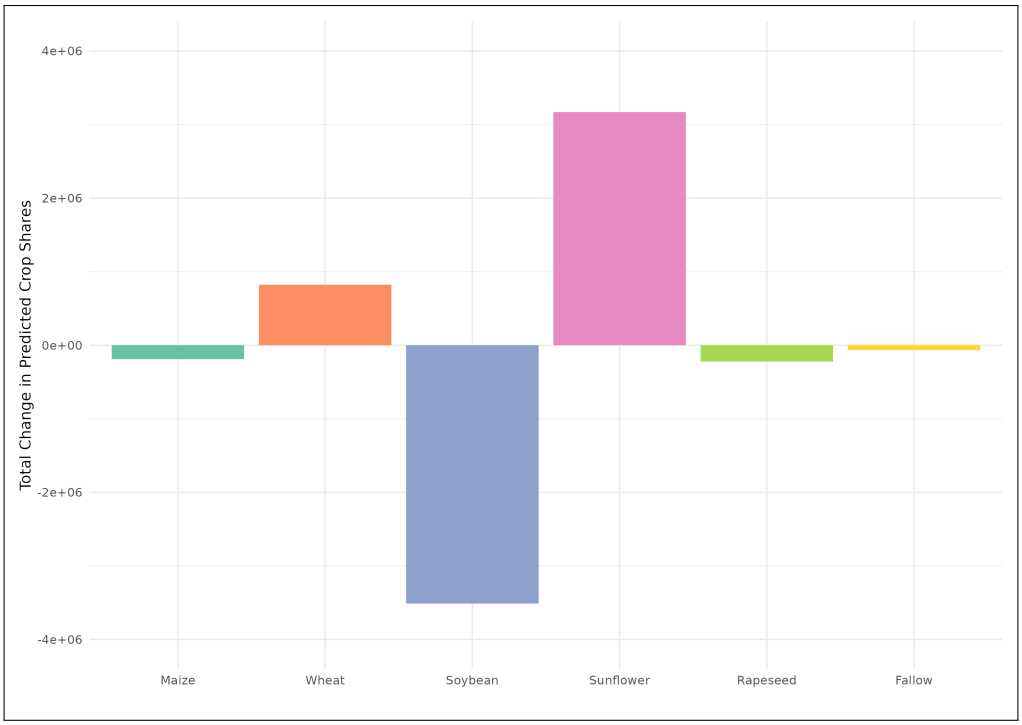

Figure 1.7 Change in Predicted Crop Shares under Climate + Yield and Market Adjustment Scenario from 2040-2070 relative to Baseline (2018-2022). This figure shows projected changes in crop shares when both climate, yields and prices evolve over time. Predicted profits are now derived from field-level yields multiplied by predicted prices, net of baseline costs. Results show smaller decine in maize share and smaller increase in wheat and sunflower shares.

An interesting finding is that across all three scenarios, the decline in soybean shares remains largely unchanged. This is because the main driver of chanage in soybean share is climate, rather than yields. As shown in Figure 1.8, the distribution of soybean yield changes is highly symmetric, with overall yields projected to increase modestly—by about 2% on average. This contrasts sharply with other crops, whose yield changes are more widely dispersed. Consequently, accounting for yield and price shocks has little effect on soybean shares.

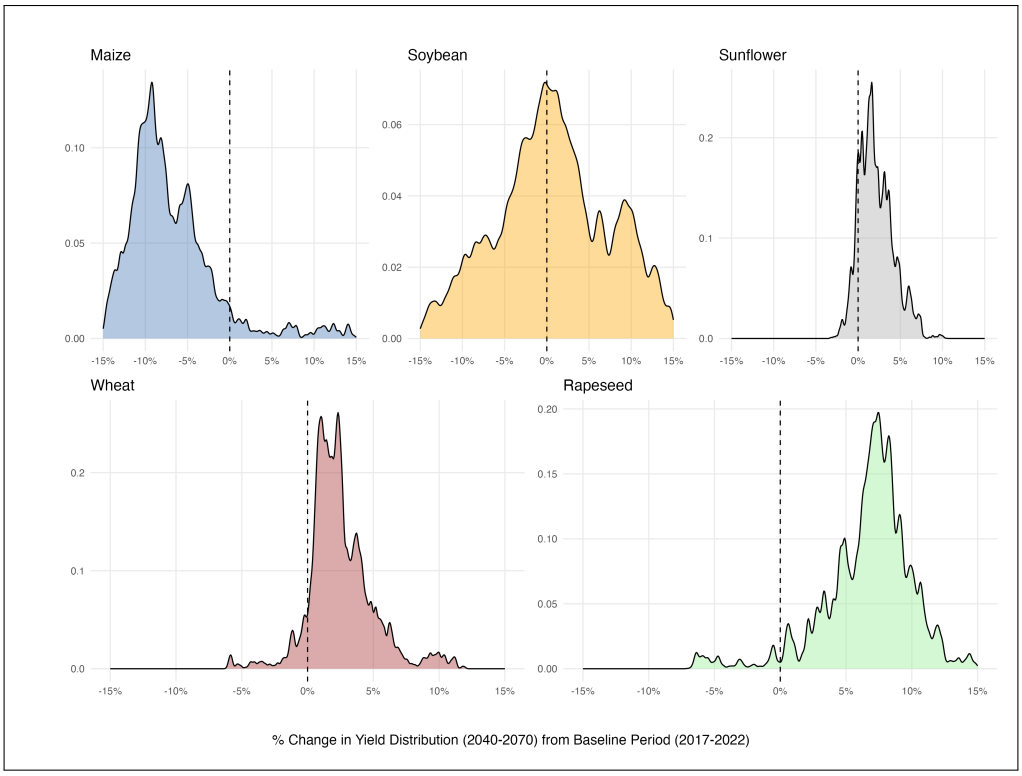

Figure 1.8 Distribution of Projected Yield Changes (2040–2070) Relative to Baseline (2017–2022). This figure presents the estimated distributions of percentage changes in yields for six major crops (Maize, Soybean, Sunflower, Wheat, Rapeseed) under future climate scenarios for the period 2040–2070, relative to the historical baseline (2017–2022). Each panel shows the kernel density distribution of projected yield changes, with the vertical dashed line indicating zero change. The results suggest substantial variation in expected yield impacts across crops. For example, while sunflower and wheat display a greater probability of yield increases, maize and rapeseed are more likely to experience yield declines.

Finally, the small decrease in fallow land observed across all three simulations suggests that farmers are more likely to adapt by switching to resilient crops rather than abandoning cultivation. This is consistent with baseline data, where only 0.4% of fields were left fallow between 2018 and 2022.

1.5.5 Welfare Implications of Crop Substitution (*forthcoming*)

Crop choices adjust meaningfully as climate and market conditions evolve. Our simulations indicate a shift away from maize and soybean to sunflower and wheat. This reallocation has economic consequences because, under baseline conditions, maize and soybean are roughly 1.5× more profitable compared to wheat and sunflower. Hence, switching to wheat and sunflower can

reduce expected profits, implying welfare costs.

Welfare is proxied by expected profits. We decompose the climate impact into: (i) direct climate losses under a no-switching counterfactual (holding farmer's baseline crop fixed and comparing its profit under climate change vs. baseline), and (ii) substitution gains from re-optimizing crop choice under climate (the increase in expected profit from reallocating across crops, relative to staying with the baseline crop under climate change). We also plan to report an offset ratio to quantify the extent to which crop switching offsets climate damages.

1.6 Conclusion

Climate change is increasingly altering weather patterns, impacting the suitability of crops traditionally grown in specific regions. Our study examines how farmers adjust their crop choices under evolving climatic and market conditions. Using rich field-level data on crop yields and crop choices, we identify the factors that shape crop choices and simulate substitution patterns under changes to short-term weather, long-term climate and expected crops' profitability. First, we estimate yield weather regression models using two-way fixed effects for five crops in our data including maize, soybean, sunflower, wheat and rapeseed. The purpose of the yield model is: (1) to identify crop-specific threshold of extreme temperatures, (2) to predict yields under climate change, and (3) to estimate future crop profitability. Results from the yield weather model are then integrated into a crop choice model to identify the key variables influencing farmers' decisions and simulate how crop choices would evolve under "climate-change only", " climate + yield", and "climate + yield and market adjustment" scenarios.

Our yield-weather model reveals crop-specific thresholds for extreme weather. For example, maize and sugar beet yields decline at temperatures below 4 and above 34°C, whereas winter crop yields decline at temperatures above 28°C. Results from yield simulations indicate significant heterogeneity in yield responses across crops and fields. Maize is predicted to experience significant decline in yields whereas soybean, wheat, and sunflower may see modest gains. Our crop choice model shows, unsurprisingly, that profitability positively influences crop choice. Increase in the incidence of spring heat stress reduces the probability of planting all crops, with farmers leaving

land fallow. Long-term climatic trends also play a significant role with wetter conditions proving to be conducive for production of maize, soybean, and wheat. Our simulations reveal substantial crop switching to mitigate losses incurred under changing climatic conditions with farmers switching away from profitable maize and soybean to the more resilient sunflower and wheat.

The vulnerability of the agricultural sector to climate change has raised interest on understanding how crop choices adapt under future climate scenarios. Our study benefits from being the first to study field-level farmers' crop choices and yields across Serbia, as well as being one of the largest, high-resolution studies of its type. Results from our estimations provide insights on how market conditions interact with climatic factors to determine cropping decisions and how these choices adjust under future market and climate scenarios. These findings highlight the critical need to support farmers' adaptive capacity—through investment in climate-resilient crop varieties, market infrastructure, and agricultural extension—so that they can respond dynamically to evolving risks. From a policy perspective, our findings suggest several directions for supporting adaptation more effectively. First, well-designed price incentives can help buffer farmers against income losses by ensuring that the transition toward less water-intensive or climate-resilient crops remains economically viable. Second, strengthening markets for lower-profitability crops through better storage, processing, and distribution systems can stabilize returns and reduce risk. Finally, targeted irrigation investments or investments in drought-resistant varieties can enable continued cultivation of high-value crops in regions most vulnerable to rainfall variability, complementing adaptation through diversification. Together, these measures can reduce welfare losses from climate change, improve agricultural resilience, and promote more equitable outcomes for farmers operating under climate stress. Future research should also explore barriers to adaptation, as even the partial adjustment observed here depends on farmers' awareness, access to new technologies, and functioning markets.

APPENDIX A

APPENDIX FOR "WEATHERING THE CHANGE: MODELING CROP CHOICES IN RESPONSE TO CLIMATE VARIABILITY"

A.1 Data Construction

A.1.1 Creating Field-level Yield Data

To construct consistent field-level yield estimates for crops over time, we extract annual raster-based yield data for five key crops: maize, soybean, sunflower, wheat, and oilseed rape. For each crop, we utilize spatial raster layers corresponding to each year from 2017 to 2022. These raster layers contain gridded estimates of crop-specific yields across the study region.

First, we overlay the raster layer data with a cadastral map of field boundaries in Serbia. Next, we compute the annual field-level yield for each polygon by extracting the weighted average yield from the corresponding raster layer. Specifically, for each field (i.e., polygon), we calculate a weighted average of the raster cell values that intersect the field, using the fraction of each raster cell that lies within the field boundary as a weight. This approach accounts for the fact that field boundaries do not perfectly align with the underlying raster grid. Rather than assigning a single raster cell's value to a field, this method leverages all intersecting cells and assigns more weight to those with greater spatial overlap. If no valid (i.e., non-missing) yield values are found within a field, the corresponding yield value is recorded as missing. Missing yields are mostly found for fields classified into non-agricultural land. However, if any raster cells within the field boundaries have missing data indicating that no crop was planted, they are ignored in the weighted average calculations. This extraction results in a panel of annual yield estimates for each field and crop.

A.1.2 Creating Field-level Crop Data

Crop classification maps for the years 2018 through 2021 were obtained as spatial datasets with each raster layer representing spatially explicit crop types for a given year. To generate field-level crop choice data, a cadastral shapefile containing field boundaries was overlaid onto the crop maps. This step obtained crop types for each intersecting field polygons. Because a field polygon may intersect multiple raster pixels with varying crop classifications, we assigned the dominant crop

type to each polygon by identifying the crop planted on the majority of pixels contained within the field's boundary.

As some crops are traditionally planted as secondary or intercropped varieties, aggregating from pixel-level data to the field level using the majority crop type may under-represent these secondary crops. To ensure that such crop-specific bias is not present in our analysis, we compare the percentage share of crops covered under pixel vs field-level data. The results are presented in Table 1. From the table, it can be observed that the crop shares under both units of analysis are very similar. However, discrepancies are more pronounced for more commonly planted crops. That said, we are not overly concerned about this potential bias, as monocropping is prevalent in Serbia (Jachia and Milovanović, 2022). In fact, 87% of fields in our data are classified into the crop category that covers more than 85% of the pixels within the field boundary.

Crop	**Pixel-Level (%)**	**Field-Level (%)**
Maize	16	19
Soybean	6	5
Sunflower	6	7
Wheat	11	12
Rapeseed	1	1

Table A.1 Percentage Share of Crops Planted by Unit of Analysis. To compare crop shares between pixel-level and field-level data (2018-2021), we first calculate pixel-level shares by summing pixels for each crop category across all years, then dividing by the total number of pixels. For field-level shares, each field is classified based on the crop occupying the majority of its pixels, and shares are computed similarly. Crops shares are similar at pixel vs more aggregated field-level data. Only maize has slightly higher representation in the field data as compared to the pixel-level data.

To obtain our final dataset, we drop sugar beet and "other crops" from our dataset. We also exclude all non-agricultural land from our dataset. Table 2 below shows the yearly classification of fields across the crop type categories. Field crops include maize, wheat, soybean, sunflower and rapeseed.

Year	Field Crops	Sugar beet	Other crops
2018	79	2	19
2019	67	1.5	31
2020	70	1	29
2021	66	0.6	33
2022	64	0.9	35

Table A.2 Classification of Fields by Crop Type and Year (Percentage Shares). This table summarizes the share of fields classified as field crops, sugar beet, and other crops for each year from 2018 to 2022. To construct the table, we used our field-level crop data from 2018 to 2022 to calculate the percentage of fields falling into each crop category by year. Field crops include maize, wheat, soybean, sunflower, and rapeseed, while all other classifications are grouped as "other crops. The share of “other crops” is growing over time whole the share of sugar beet is declining over time. This acts as a justification to dropping these 2 crop categories from our final dataset..

From Table 2, it is evident that fields classified as “other crops” exhibit an upward trend with a steady increase from 2018 to 2022. Among fields classified as “other crops”, approximately 14% of these fields were consistently categorized as ’other crops’ across all five years. Additionally, only 10% of these fields were classified in the “other crops category” in only one year. This high degree of persistence suggests that a significant share of fields classified as “other crops” are likely perennial and unlikely to rotate within typical annual cropping cycles. Moreover, the heterogenous nature of this category - with no way to distinguish whether a field classified as other crops has a high-value or a low-value crop planted on it - introduces significant measurement error in the analysis. Given this ambiguity, we exclude observations for a field in the year it is classified as “other crops”.

A.1.3 Creating Field-level Temperature Data

To assign our temperature variables to the fields in our data, we intersect gridded temperature data in raster format with the cadastral map of field boundaries. For each year, temperature rasters representing hours of exposure in different temperature bins are generated from interpolated daily temperature data and utilized in the yield model. Similarly, temperature rasters with average and extreme temperatures are constructed for the crop choice model.

Using spatial extraction tools, temperature values from temperature raster cells are assigned to

the field polygons. Because field boundaries often overlap multiple temperature raster cells, we compute temperature metrics as weighted averages. Rather than assigning the value of a single cell to a field, we calculate weighted averages of temperature variables for each field polygon, where the weights represent the proportion of each raster cell that overlaps the polygon.

Approximately 4% of field polygons do not intersect with temperature raster cells. We utilize Inverse Distance Weighting (IDW) using the ten nearest neighboring fields to assign temperature values to these fields. Missing values are estimated as weighted averages of neighboring observations, where weights decrease with distance, assigning higher weights to geographically closer observations. While the choice of ten neighbors is arbitrary, we assess robustness by repeating the imputation with five and twenty neighbors. The resulting values remain identical in terms of mean, minimum, and maximum temperature, suggesting that our findings are not sensitive to the specific imputation parameter.

A.1.4 Creating Field-level Soil Moisture Data

The spatial extent of the SWAT+ model includes the watershed of the Danube River and its tributaries. The watershed is divided into subbasins, and outputs obtained from the model are at the subbasin level. This indicates that the soil moisture data used in this analysis is at a more aggregated subbasin-level rather than at the field-level. To assign soil moisture to our field data, we intersect the soil moisture polygons with the map of field boundaries. This intersection, however, leads to duplication as field polygon intersects with multiple soil moisture polygons. To address this, we compute a weighted average of soil moisture values for each field, weighting by the area of overlap. Larger overlaps thus have a proportionally greater influence on the field-level soil moisture averages.

A.1.5 Creating Field-level Soil Quality Data

To construct soil quality variable, we obtain data on soil raster layers along with corresponding soil attribute information including available water capacity from Harmonized World Soil Database (Fischer et al., 2008). The soil raster data is overlaid onto the cadastral shapefile containing field boundaries, and each field polygon is assigned the soil type covering the largest portion of its area.

Soil attributes are then linked to fields via soil type identifiers. Because each soil type corresponds to multiple soil layers with varying properties, a direct merge leads to duplicate entries. To assign a single AWC value to a field polygon, we take an average across all layers. While a weighted average would be ideal, due to the lack of spatial information such an approach is not feasible.

A.1.6 Estimating the Yield–Price Relationship

To identify how local yield shocks affect crop prices, we estimate a regression of log domestic prices on log yields using national-level data from 2006–2023 (FAO, 2025a,b). We control for world prices (IMF, 2025), as well as year and crop fixed effects. World prices are controlled for as Serbia is a price taker - domestic prices are strongly influenced by international commodity markets. Controlling for world prices helps ensure that the estimated relationship captures supply-driven, rather than market-wide, effects.

To address the endogeneity of yields, we adopt an instrumental variables approach using national soil-moisture anomalies and temperature as instruments for yields. These variables are aggregated to the national level by averaging growing-season values across all subbasins (for soil moisture) and grid cells (for temperature). These instruments are plausibly relevant (weather affects yields) and satisfy the exclusion restriction as national weather shocks influence crop prices primarily through yields. Our results show that a 1% increase in yields decreases crop prices by 0.42% and the effect is statistically significant at the 5% level. In addition, the F-statistic for instrument relevance is 11.14 (p-value < 0.001). This value exceeds the conventional threshold of 10, indicating that the instruments are not weak. A Sargan over-identification test (stat = 1.306, p-value = 0.253) provides no evidence against instrument validity.

A.2 Descriptive Statistics

Variable	Mean	SD	Min	Max
2018–2022				
Profits (dinars/ha)	62,521	39,308	0	157,000
29-year Historical Spring Temperature (°C)	18.98	0.34	17.33	20.09
29-year Historical Soil Moisture (mm)	89.23	24.97	5.78	247.50
Spring Heat Stress Days (hours)	80.32	67.07	0	244.25
Spring Cold Stress Days (hours)	169.26	47.67	38.75	265.00
Winter Heat Stress Days (hours)	51.69	37.39	0	149.25
Winter Cold Stress Days (hours)	128.96	113.76	0	442.50
Spring Soil Moisture Anomalies	-0.46	0.45	-1.72	1.77
2041–2045				
29-year Historical Spring Temperature (°C)	19.28	0.32	18.43	20.19
29-year Historical Soil Moisture (mm)	76.85	20.34	4.79	222.02
Spring Heat Stress Days (hours)	145.41	41.05	68.95	246.05
Spring Cold Stress Days (hours)	184.45	39.00	98.00	285.95
Winter Heat Stress Days (hours)	33.39	13.16	10.90	73.25
Winter Cold Stress Days (hours)	149.92	60.67	30.75	315.80
Spring Soil Moisture Anomalies	-0.25	0.41	-1.92	1.44
2046–2050				
29-year Historical Spring Temperature (°C)	19.41	0.32	18.57	20.30
29-year Historical Soil Moisture (mm)	76.48	19.50	4.68	215.46
Spring Heat Stress Days (hours)	108.04	32.91	48.20	199.35
Spring Cold Stress Days (hours)	179.88	20.22	127.85	245.85
Winter Heat Stress Days (hours)	42.97	18.06	16.05	90.45
Winter Cold Stress Days (hours)	200.97	69.68	64.80	361.15

Table A.3 (continued)

Variable	Mean	SD	Min	Max
Spring Soil Moisture Anomalies	-0.06	0.30	-1.13	1.53
2051–2055				
29-year Historical Spring Temperature (°C)	19.52	0.32	18.69	20.42
29-year Historical Soil Moisture (mm)	79.28	19.87	4.69	217.88
Spring Heat Stress Days (hours)	122.15	40.73	54.60	258.20
Spring Cold Stress Days (hours)	142.37	39.23	80.55	254.75
Winter Heat Stress Days (hours)	45.32	25.91	11.45	123.50
Winter Cold Stress Days (hours)	185.05	66.62	62.90	315.70
Spring Soil Moisture Anomalies	-0.22	0.33	-1.49	0.91
2056–2060				
29-year Historical Spring Temperature (°C)	19.66	0.32	18.83	20.55
29-year Historical Soil Moisture (mm)	79.75	19.78	4.61	218.76
Spring Heat Stress Days (hours)	150.58	32.29	86.05	236.20
Spring Cold Stress Days (hours)	202.86	60.97	93.30	343.75
Winter Heat Stress Days (hours)	33.02	10.67	8.75	58.15
Winter Cold Stress Days (hours)	152.65	78.14	26.90	348.70
Spring Soil Moisture Anomalies	-0.08	0.55	-1.89	2.07
2061–2065				
29-year Historical Spring Temperature (°C)	19.76	0.33	18.91	20.67
29-year Historical Soil Moisture (mm)	82.77	20.40	4.49	220.83
Spring Heat Stress Days (hours)	146.02	28.78	86.30	223.10
Spring Cold Stress Days (hours)	204.58	43.20	86.15	293.65
Winter Heat Stress Days (hours)	27.79	10.09	2.95	56.45
Winter Cold Stress Days (hours)	183.13	35.00	104.05	273.05

Table A.3 (continued)

Variable	Mean	SD	Min	Max
Spring Soil Moisture Anomalies	0.08	0.50	-1.53	1.98
2066–2070				
29-year Historical Spring Temperature (°C)	19.90	0.33	19.06	20.77
29-year Historical Soil Moisture (mm)	82.82	20.75	4.41	222.19
Spring Heat Stress Days (hours)	135.06	51.43	61.10	295.40
Spring Cold Stress Days (hours)	203.43	70.41	69.65	363.20
Winter Heat Stress Days (hours)	32.33	12.90	5.70	64.75
Winter Cold Stress Days (hours)	109.09	33.13	51.45	198.25
Spring Soil Moisture Anomalies	0.09	0.41	-1.19	2.00

Table A.3 Descriptive Statistics

A.3 Regression Results

Variable	Maize	Soybean	Sunflower
temp_neg2_to_1	0.004***	-0.002***	-0.00075***
	(0.0004)	(0.00054)	(0.00025)
temp_1_to_4	-0.001**	0.00052*	0.0000452
	(0.0002)	(0.0003)	(0.00022)
temp_4_to_7	0.0005***	0.001***	0.00041**
	(0.0002)	(0.00024)	(0.00019)
temp_7_to_10	0.0017***	0.002***	0.00087***
	(0.0001)	(0.00015)	(0.00021)
temp_10_to_13	0.0022***	0.0048***	0.00076***
	(0.0002)	(0.0003)	(0.00022)
temp_13_to_16	0.0018***	0.00422***	0.00072***
	(0.00011)	(0.00015)	(0.00014)
temp_19_to_22	0.00014	0.00076***	0.00031**
	(0.00013)	(0.00018)	(0.00014)
temp_22_to_25	0.0006***	0.00424***	0.0013***
	(0.00015)	(0.0002)	(0.00014)
temp_25_to_28	0.0039***	0.005***	0.001***
	(0.00012)	(0.00017)	(0.00015)
temp_28_to_31	0.00022*	0.00097***	0.00016
	(0.00012)	(0.0002)	(0.00015)
temp_31_to_34	-0.000489***	-0.00066**	0.00039**
	(0.00014)	(0.00028)	(0.00019)
temp_34_to_37	-0.0024***	-0.0034***	0.00065***
	(0.0002)	(0.00018)	(0.00019)
temp_37_to_40	-3.10e-05	-0.0074***	0.0012***
	(0.0004)	(0.00035)	(0.00028)
early_season_soil	1.62e-05	-0.00036***	0.00046***
	(0.0001)	(0.00011)	(9.09e-05)
growing_soil	0.001***	0.0013***	0.00027**
	(0.00017)	(0.00021)	(0.00013)
harvesting_soil	-0.002***	-0.0027***	-0.00055***
	(0.00014)	(0.00021)	(0.00011)
Constant	-2.120***	-8.709***	-1.902***
	(0.253)	(0.502)	(0.550)
Observations	11,158,548	11,157,990	11,158,548
Number of id	1,859,758	1,859,665	1,859,758
R-squared	0.901	0.952	0.333

Table A.4 Yield Weather Regression Model Results for Spring Crops.

Robust (clustered by municipality) standard errors are in the parentheses.
*** $p < 0.01$, ** $p < 0.05$, * $p < 0.1$.

Variable	Wheat	Rapeseed
temp_neg8_to_neg5	0.00075***	0.0012***
	(5.60e-05)	(8.71e-05)
temp_neg5_to_neg2	0.00088***	0.0007***
	(7.35e-05)	(0.00016)
temp_neg2_to_1	0.0006***	0.0012***
	(6.16e-05)	(9.22e-05)
temp_1_to_4	0.00057***	0.00056***
	(5.62e-05)	(8.92e-05)
temp_4_to_7	0.00046***	0.00055***
	(6.90e-05)	(0.00011)
temp_7_to_10	0.00071***	0.00097***
	(4.09e-05)	(9.19e-05)
temp_10_to_13	0.0008***	0.00018
	(7.00e-05)	(0.00011)
temp_13_to_16	0.00036***	0.00047***
	(9.01e-05)	(0.00014)
temp_19_to_22	0.00041***	0.0007***
	(8.52e-05)	(0.00018)
temp_22_to_25	0.00063***	0.0018***
	(6.52e-05)	(0.00017)
temp_25_to_28	0.0015***	-0.00093***
	(0.000126)	(0.00024)
temp_28_to_31	-0.00068***	-0.0004***
	(5.90e-05)	(0.00013)
early_season_soil	-0.0013***	-0.0003**
	(7.72e-05)	(0.00012)
growing_soil	0.00052***	0.00052***
	(7.29e-05)	(0.00014)
harvesting_soil	0.00024***	4.44e-05
	(5.28e-05)	(9.98e-05)
Constant	-1.656***	-2.62***
	(0.332)	(0.587)
Observations	12,071,556	11,158,548
Number of id	2,011,926	1,859,758
R-squared	0.719	0.746

Table A.5 Yield Weather Regression Model Results for Winter Crops.

Robust (clustered by municipality) standard errors are in the parentheses.
*** $p < 0.01$, ** $p < 0.05$, * $p < 0.1$.

Variable	**Conditional Logit**				
Lagged Profits (Inflated)			9.35e-06***		
			(2.35e-06)		
Crop-Specific Results	Maize	Soybean	Sunflower	Wheat	Rapeseed
Spring Season Heat Stress	-0.0015**	-0.0023***	-0.0057***	-0.0014**	-0.00046
	(0.0005)	(0.0007)	(0.0009)	(0.0006)	(0.0016)
Winter Season Heat Stress	0.0021**	0.0069***	0.0081***	0.0041***	-0.00028
	(0.001)	(0.001)	(0.0009)	(0.0008)	(0.0012)
Spring Season Cold Stress	-0.0079***	-0.0126***	0.014	0.0034	-0.0076
	(0.0029)	(0.0041)	(0.0031)	(0.0027)	(0.0048)
Winter Season Cold Stress	-0.0015	-0.0014	-0.005***	-0.0021**	0.001
	(0.0009)	(0.0013)	(0.0011)	(0.001)	(0.0019)
29-yr Moving Avg Spring Temp	1.37***	-1.8***	2.41***	1.28***	-0.53
	(0.18)	(0.31)	(0.23)	(0.20)	(0.34)
Spring Season Soil Moisture Anomalies	-0.30***	-0.69***	0.17	0.022	-0.45***
	(0.10)	(0.13)	(0.11)	(0.10)	(0.17)
29-yr Moving Avg Spring Soil Moisture	0.0042*	0.016***	-0.00065	0.0017	-0.011**
	(0.0022)	(0.0023)	(0.002)	(0.20)	(0.005)
Field Area	6.02e-06	6.48e-06	6.60e-06	6.31e-06	7.72e-06
	(8.28e-06)	(8.27e-06)	(8.27e-06)	(8.28e-06)	(8.30e-06)
Available Water Capacity (AWC)	13.29***	8.61***	7.74***	7.46***	19.10***
	(1.46)	(2.44)	(1.38)	(1.36)	(4.24)
Elevation	0.0034*	-0.0465***	0.0121***	0.0017	-0.00018
	(0.0010)	(0.0041)	(0.0021)	(0.0018)	(0.0028)
Irrigation	2.01***	2.48***	0.87***	1.42***	1.74***
	(0.29)	(0.31)	(0.30)	(0.28)	(0.32)
Time Trend	0.0080	0.37***	-0.39***	-0.11	0.32
	(0.09)	(0.13)	(0.11)	(0.10)	(0.20)
Constant	-24.17***	37.72***	-45.27***	-22.32***	9.19
	(3.67)	(6.11)	(4.65)	(4.02)	(6.72)

Table A.6 Conditional Logit Results by Crop.

Baseline option is leaving land fallow. All coefficients are relative to land left fallow.
Coefficients on field attributes and crop-specific coefficients are not included in the Table.
Robust (clustered by municipality) standard errors are in the parentheses.
*** $p < 0.01$, ** $p < 0.05$, * $p < 0.1$.

Variable	**Conditional Logit**				
Lagged Profits (Inflated)			4.42e-06*		
			(2.33e-06)		
Crop-Specific Results	Maize	Soybean	Sunflower	Wheat	Rapeseed
Spring Season Heat Stress	0.0026***	0.0013	-0.0007	0.0031***	0.0062***
	(0.0008)	(0.0009)	(0.0011)	(0.0008)	(0.0017)
Winter Season Heat Stress	0.0015	0.0055***	0.0069***	0.0022*	-0.0025
	(0.0013)	(0.0013)	(0.0012)	(0.0012)	(0.0016)
Spring Season Cold Stress	-0.0115***	-0.0118***	0.0132***	-0.0043	-0.0168***
	(0.0030)	(0.0039)	(0.0031)	(0.0026)	(0.0046)
Winter Season Cold Stress	-0.0003	-0.0004	-0.0051***	-0.0007	0.0030*
	(0.0010)	(0.0014)	(0.0012)	(0.0010)	(0.0018)
29-yr Moving Avg Spring Temp	0.6890***	-2.0660***	1.5410***	0.2130	-1.3750***
	(0.1540)	(0.2680)	(0.2050)	(0.1720)	(0.3230)
Spring Season Soil Moisture Anomalies	-0.1560	-0.4330***	0.4100***	0.0746	-0.4140**
	(0.0976)	(0.1340)	(0.1150)	(0.1020)	(0.1690)
29-yr Moving Avg Spring Soil Moisture	0.0020	0.0145***	-0.0014	0.0008	-0.0085**
	(0.0015)	(0.0016)	(0.0015)	(0.0015)	(0.0041)

Table A.7 (continued)

Crop-Specific Results	Maize	Soybean	Sunflower	Wheat	Rapeseed
Field Area	-3.9e-07	4.1e-07	3.7e-07	-1.6e-07	1.4e-06*
	(7.8e-07)	(7.7e-07)	(7.6e-07)	(7.7e-07)	(7.7e-07)
Available Water Capacity (AWC)	11.7100***	4.4850**	3.8980***	4.5990***	19.0700***
	(1.4570)	(2.1060)	(1.2760)	(1.3380)	(4.0890)
Elevation	0.0009	-0.0466***	0.0045**	-0.0051***	-0.0055*
	(0.0017)	(0.0037)	(0.0019)	(0.0019)	(0.0029)
Irrigation	1.5450***	1.9270***	0.4170*	1.0520***	1.5000***
	(0.2460)	(0.2560)	(0.2480)	(0.2360)	(0.2830)
Time Trend	0.1310	0.3210***	-0.4300***	0.0434	0.5590***
	(0.0910)	(0.1210)	(0.1110)	(0.1000)	(0.1830)
1.crop_lag	0.7790***	-0.8700***	-0.3140***	-0.4110***	3.4430***
	(0.1010)	(0.1080)	(0.1110)	(0.1070)	(0.1430)
2.crop_lag	1.0740***	0.5380***	-1.3430***	0.2720**	0.6300**
	(0.1040)	(0.1480)	(0.1180)	(0.1150)	(0.3010)
3.crop_lag	0.4420***	-0.5650***	-0.8860***	0.0637	0.3790*
	(0.1330)	(0.1730)	(0.1590)	(0.1360)	(0.2150)
4.crop_lag	1.2840***	-1.1440***	-0.8410***	2.2660***	2.2430***

Table A.7 (continued)

Crop-Specific Results	Maize	Soybean	Sunflower	Wheat	Rapeseed
	(0.1260)	(0.1250)	(0.1320)	(0.1170)	(0.1850)
5.crop_lag	1.6530***	-0.0041	0.2700	2.3270***	4.5400***
	(0.2850)	(0.2840)	(0.2700)	(0.2660)	(0.2920)
6.crop_lag	-1.9080***	-3.5180***	-2.9840***	-1.9440***	-0.9680***
	(0.0880)	(0.0950)	(0.1070)	(0.0950)	(0.1530)
20.crop_lag	-7.1120***	-8.1080***	-8.2640***	-7.0180***	-7.2340***
	(0.1170)	(0.2100)	(0.1290)	(0.1080)	(0.4630)
Constant	-9.6330***	45.3600***	-26.0300***	0.5120	25.0600***
	(3.0800)	(5.2720)	(4.1460)	(3.4950)	(6.3670)

Table A.7 Conditional Logit Results by Crop (Including Lagged Crops).

Baseline option is leaving land fallow. All coefficients are relative to land left fallow.

Coefficients on field attributes and crop-specific coefficients are not included in the Table.

Robust (clustered by municipality) standard errors are in the parentheses.

*** $p < 0.01$, ** $p < 0.05$, * $p < 0.1$.

BIBLIOGRAPHY

Agroberichten Buitenland (2020). Soybean cultivation in serbia. https://www.agroberichtenbuitenland.nl/actueel/nieuws/2020/07/15/soy-cultivation-in-serbia. Accessed: August 2025.

Agroberichten Buitenland (2024). Serbia: First results of agriculture census show major shifts. https://www.agroberichtenbuitenland.nl/actueel/nieuws/2024/02/02/serbia-census. Accessed: August 2025.

Ahmed, M. H., Tesfaye, W. M., and Gassmann, F. (2023). Early growing season weather variation, expectation formation and agricultural land allocation decisions in ethiopia. *Journal of Agricultural Economics*, 74:255–272.

Arora, G., Feng, H., Anderson, C. J., and Hennessy, D. A. (2020). Evidence of climate change impacts on crop comparative advantage and land use. *Agricultural Economics*, 51(2):221–236.

BioSense Institute (2022). Survey of farmers. https://biosens.rs/en/institute.

Copernicus European Drought Observatory (2019). *Soil Moisture Anomaly (SMA) Indicator Factsheet*. European Commission. Available at: https://drought.emergency.copernicus.eu/data/factsheets/factsheet_soilmoisture.pdf (accessed: 2025-10-18).

Cornes, R., der Schrier, G. V., den Besselaar, E. J. V., and Jones, P. D. (2018). An ensemble version of the e-obs temperature and precipitation data sets. *Journal of Geophysical Research Atmospheres*, 123.

Cui, X. (2020). Climate change and adaptation in agriculture: evidence from us cropping patterns. *Climate change and adaptation in agriculture: Evidence from US cropping patterns*, 101.

de Perez, E. C., Ganapathi, H., Masukwedza, G. I., Griffin, T., and Kelder, T. (2023). Potential for surprising heat and drought events in wheat-producing regions of usa and china. *npj Climate and Atmospheric Science*, 6.

Debaeke, P., Casadebaig, P., Flenet, F., and Langlade, N. (2017). Sunflower crop and climate change: vulnerability, adaptation, and mitigation potential from case-studies in europe. *OCL - Oilseeds and Fats, Crops and Lipids*, 24.

Dodig, D., D.Rancic, Radovic, B., M.Zoric, J.Savic, V.Kandic, I.Pecinar, S.Stanojevic, A.Seslija, D.Vassilev, and S.Peckic-Quarrie (2017). Response of wheat plants under post-anthesis stress induced by defoliation: Ii. contribution of peduncle morpho-anatomical traits and carbon reserves to grain yield. *The Journal of Agricultural Science*, 155:457–493.

Dosio, A. (2016). Projections of climate change indices of temperature and precipitation from an ensemble of bias-adjusted high-resolution euro-cordex regional climate models. *Journal of Geophysical Research: Atmospheres*, 121:5488–5511.

European Environment Agency (2019). European digital elevation model. https://www.eea.europa.eu/en/datahub/datahubitem-view/d08852bc-7b5f-4835-a776-08362e2fbf4b. Accessed: March 2024.

FAO (2023). Mitigating the impacts of climate change in serbian agriculture. https://www.fao.org/countryprofiles/news-archive/detail-news/en/c/1640481/. Accessed: 2025-08-26.

FAO (2025a). Crops and livestock products. https://www.fao.org/faostat/en/#data/QCL. Accessed: July 2025.

FAO (2025b). Producer prices. https://www.fao.org/faostat/en/#data/PP. Accessed: April 2025.

Fischer, G., Nachtergaele, F. O., Prieler, S., van Velthuizen, H., Verelst, L., and Wiberg, D. (2008). Global agro-ecological zones assessment for agriculture (gaez 2008). Technical report, IIASA and FAO, Laxenburg, Austria and Rome, Italy.

Heikonen, S., Heino, M., Jalava, M., Siebert, S., Viviroli, D., and Kummu, M. (2025). Climate change threatens crop diversity at low latitudes. *Nature Food*, 6:331–342.

Hoang, T. A., Nachtergaele, F., F.Chiozza, and Ziadat, F. (2022). Land suitability for crop production in the future: Solaw21 technical background report. Technical report, FAO.

IMF (2025). Primary commodity prices. https://www.imf.org/en/Research/commodity-prices. Accessed: September 2025.

International Trade Administration (2024). Serbia country commercial guide: Agricultural sectors. https://www.trade.gov/country-commercial-guides/serbia-agricultural-sectors. Accessed: 2025-08-26.

Jachia, L. and Milovanović, J. (2022). Thematic update sustainable food systems. Technical report, UN Serbia.

Jalali, J., Bhattarai, N., Greene, J., Liu, T., Marko, O., Radulović, M., Sears, M., and Woznicki, S. A. (2025). Climate change threatens water resources for major field crops in the serbian danube river basin by the mid-21st century. *Journal of Hydrology: Regional Studies*, 59.

Jeločnik, M., Zubović, J., and Zdravković, A. (2019). Estimating impact of weather factors on wheat yields by using panel model approach — the case of serbia. *Agricultural Water Management*, 221:493–501.

Kandel, H. and Knodel, J. (2021). Canola production. Technical report, North Dakota State University Extension.

Kresovic, B., Matovic, G., Gregoric, E., Djuricin, S., and Bodroza, D. (2014). Irrigation as a climate change impact mitigation measure: an agronomic and economic assessment of maize production in serbia. *Agricultural Water Management*, 139:7–16.

Marković, M., Lugonja, P., Brdar, S., Živaljević, B., and Crnojević, V. (2022). Detection of double-cropping systems using machine learning and sentinel 2 imagery - a case study of bačka and srem regions, serbia. In *EGU General Assembly 2022*, Vienna, Austria.

Maslac, T. (2022). Serbia grain summer update 2022. Technical report, USDA.

McCarl, B. A., Thayer, A. W., and Jones, J. P. H. (2016). The challenge of climate change adaptation for agriculture: an economically oriented review. *Journal of Agricultural and Applied Economics*, 48:321–344.

McFadden, D. and Train, K. (2000). Mixed mnl models for discrete response. *Journal of Applied Econometrics*, 15:447–470.

Mendis, S. S., Udawatta, R. P., Anderson, S. H., Nelson, K. A., and II, R. L. C. (2022). Effects of cover crops on soil moisture dynamics of a corn cropping system. *Soil Security*, 8.

Miao, R., Khanna, M., and Huang, H. (2016). Responsiveness of crop yield and acreage to prices and climate. *American Journal of Agricultural Economics*, 98:191–211.

Mihailovic, D., Lalic, B., Drešković, N., Mimić, G., and Djurdjević, V. (2015). Climate change effects on crop yields in serbia and related shifts of köppen climate zones under the sres-a1b and sres-a2. *International Journal of Climatology*, 35:3320–3334.

Minoli, S., Jägermeyr, J., Asseng, S., Urfels, A., and Müller, C. (2022). Global crop yields can be lifted by timely adaptation of growing periods to climate change. *Nature Communications*, 13.

Mirosavljević, M., Mikić, S., Župunski, V., Abdelhakim, L., Trkulja, D., Zhou, R., Špika, A. K., and Ottosen, C.-O. (2024). Effects of heat stress during anthesis and grain filling stages on some physiological and agronomic traits in diverse wheat genotypes. *Plants*, 13.

Moniruzzaman, S. (2015). Crop choice as climate change adaptation: Evidence from bangladesh. *Ecological Economics*, 118:90–98.

Mu, J. E., Sleeter, B. M., Abatzoglou, J. T., and Antle, J. M. (2017). Climate impacts on agricultural land use in the usa: the role of socio-economic scenarios. *Climatic Change*, 144:329–345.

Ortiz-Bobea, A., Wang, H., Carrillo, C. M., and Ault, T. R. (2019). Unpacking the climatic drivers of us agricultural yields. *Environmental Research Letters*, 14.

Pandžić, M., Ljubicic, N. D., Mimić, G., Pandžić, J., and Pejak, B. (2020). A case study of monitoring maize dynamics in serbia by utilizing sentinel-1 data and growing degree days.

ISPRS Annals of the Photogrammetry Remote Sensing and Spatial Information Sciences, 3:117–124.

Radulović, M., Brdar, S., Pejak, B., Lugonja, P., Athanasiadis, I., Pajević, N., Pavić, D., and Crnojević, V. (2023). Machine learning-based detection of irrigation in vojvodina (serbia) using sentinel-2 data. *GIScience Remote Sensing*, 60.

Rising, J. and Devini, N. (2020). Crop switching reduces agricultural losses from climate change in the united states by half under rcp 8.5. *Nature Communications*, 11.

Seo, S. N. and Mendelsohn, R. O. (2008). An analysis of crop choice: adapting to climate change in south american farms. *Ecological Economics*, 67:109–116.

Sghaier, A. H., Khaeim, H., Ákos Tarnawa, Kovács, G. P., Gyuricza, C., and Kende, Z. (2023). Germination and seedling development responses of sunflower (helianthus annuus l.) seeds to temperature and different levels of water availability. *Agriculture*, 13.

Sloat, L. L., Davis, S. J., Gerber, J. S., Moore, F. C., Ray, D. K., West, P. C., and Mueller, N. D. (2020). Climate adaptation by crop migration. *Nature Communications*, 11.

Sokoto, M. B. and Singh, A. (2013). Yield and yield components of bread wheat as influenced by water stress, sowing date and cultivar in sokoto, sudan savannah, nigeria. *American Journal of Plant Sciences*, 4.

Statistical Office of the Republic of Serbia (2024). Irrigated areas of arable land by different crops. `https://data.stat.gov.rs/Home/Result/1300020302?languageCode=en-US`. Accessed: April 2025.

Tack, J., Barkley, A., and Nalley, L. L. (2015). Effect of warming temperatures on us wheat yields. *Proceedings of the National Academy of Science*, 112:6931–6936.

Tovjanin, M. J., Lalic, B., Mihailovic, D., and Jacimovic, G. (2015). mpact of climate change and carbon dioxide fertilization effect on irrigation water demand and yield of soybean in serbia. *The Journal of Agricultural Science*, 153:1365–1379.

Yu, C., Miao, R., and Khanna, M. (2021). Maladaptation of u.s. corn and soybeans to a changing climate. *Scientific Reports*, 11.

Živaljević, B., Marković, M., Mimić, G., Marko, O., and Woznicki, S. (2024). Multi-annual crop maps reveal cropping patterns in the vojvodina region (serbia). In *2th International Conference on Agro-Geoinformatics (Agro-Geoinformatics)*, Novi Sad, Serbia.